Modular Nano-Scaffold Biocatalysis for Superior PET Depolymerization and Valorization

Yujia Zhang[1,2], Chongsen Li[1,2], Ehsan Hashimi[2], Enting Xu[3], Xuemei Yang[3], Yanbing Lin[1], Hui Gao[2,*], Zhuobin Liang[2,*,+]

[1] College of Life Sciences, Northwest A&F University, Yangling, Shaanxi 712100, China

[2] Institute of Molecular Physiology, Shenzhen Bay Laboratory, Shenzhen 518132, China

[3] School of Science, Harbin Institute of Technology (Shenzhen), Shenzhen 518055, China

[+] Lead Contact

[*] Correspondence addressed to: ZL (zbliang@szbl.ac.cn) or HG (gaohui@szbl.ac.cn)

Abstract

The global crisis of polyethylene terephthalate (PET) waste demands innovative solutions for sustainable management. Current approaches are often inefficient, energy-intensive, and result in incomplete depolymerization. Here, we introduce SPEED (Scaffold-enabled PET Enzyme Ensemble-augmented Degradation), a transformative biocatalytic platform engineered for the superior degradation across diverse PET substrates. Through the strategic combination of complementary PET hydrolases on a tailored protein nano-scaffold and extensive optimization, SPEED achieves near-complete depolymerization of PET into its constituent monomers, exceeding existing biocatalytic systems' efficiency by up to two orders of magnitude. The platform's versatility and industrial relevance are further demonstrated through successful integration with metal-organic frameworks (MOFs) for enhanced stability and reusability, enabling PET upcycling into valuable products, and its compatibility with a yeast-based live cell system for surface display. SPEED's high efficiency, adaptability, and cost-effectiveness position it as a powerful technology to accelerate sustainable plastic waste management and drive a circular PET economy.

Main

Polyethylene terephthalate (PET), a ubiquitous polyester valued for its durability and versatility, poses a major sustainability crisis due to its environmental persistence and the limitations of traditional recycling. Its vast global production, exceeding 30 million tons annually, leads to widespread plastic pollution, harming terrestrial and marine ecosystems [1], releasing hazardous microplastics [2], and posing risks to human health [3,4]. Traditional mechanical recycling requires extensive sorting, often yields low-value products due to incomplete degradation [5], and can further exacerbate microplastic pollution [6]. Chemical recycling, while promising, can be energy-intensive and produce undesirable byproducts [7,8].

Biocatalytic degradation, harnessing enzymes from microorganisms to break down PET polymers, offers a promising and sustainable alternative [9]. This approach is attractive due to its potential for complete degradation, lower environmental impact, and the generation of valuable products through recycling and upcycling, as showcased in early-phase industrial demonstrations [10]. Several PET hydrolases, including TfH [11], leaf-branch cutinase (LCC) [12], and *Is*PETase [13], have been identified and further engineered [14,15] (**Supplementary Table 1**). However, existing biocatalytic systems still face major hurdles such as incomplete conversion [16], intermediate inhibition [17], limited efficiency on high-crystallinity PET, and cost-effectiveness [18], hindering their widespread industrial implementation.

Recent efforts to address these limitations have focused on multi-enzyme systems that leverage the synergistic action of different PET hydrolases [19–25] (**Table 1**). While these systems have shown promise, challenges in achieving complete depolymerization and overcoming intermediate inhibition persist. Moreover, they often lack the modularity and adaptability needed to incorporate diverse enzyme functionalities for optimal PET degradation across various substrates and conditions, and to expand into applications such as monomer upcycling and live cell systems, underscoring the need for innovative designs.

In this study, we introduce Scaffold-enabled PET Enzyme Ensemble-augmented Degradation (SPEED), a modular biocatalytic platform designed to address the PET waste crisis and promote a shift towards a circular economy (**Fig. 1**). SPEED strategically combines multiple complementary PET hydrolases with a flexible nanometric protein scaffold, fostering their synergistic action to ensure complete intermediate conversion across diverse substrates under mild conditions. Through iterative optimization, SPEED significantly outperforms existing biocatalytic systems. The platform's versatility and industrial relevance are further showcased through successful applications in MOF-immobilization, PET upcycling, and a yeast-based live cell system, highlighting its transformative potential for sustainable plastic waste management.

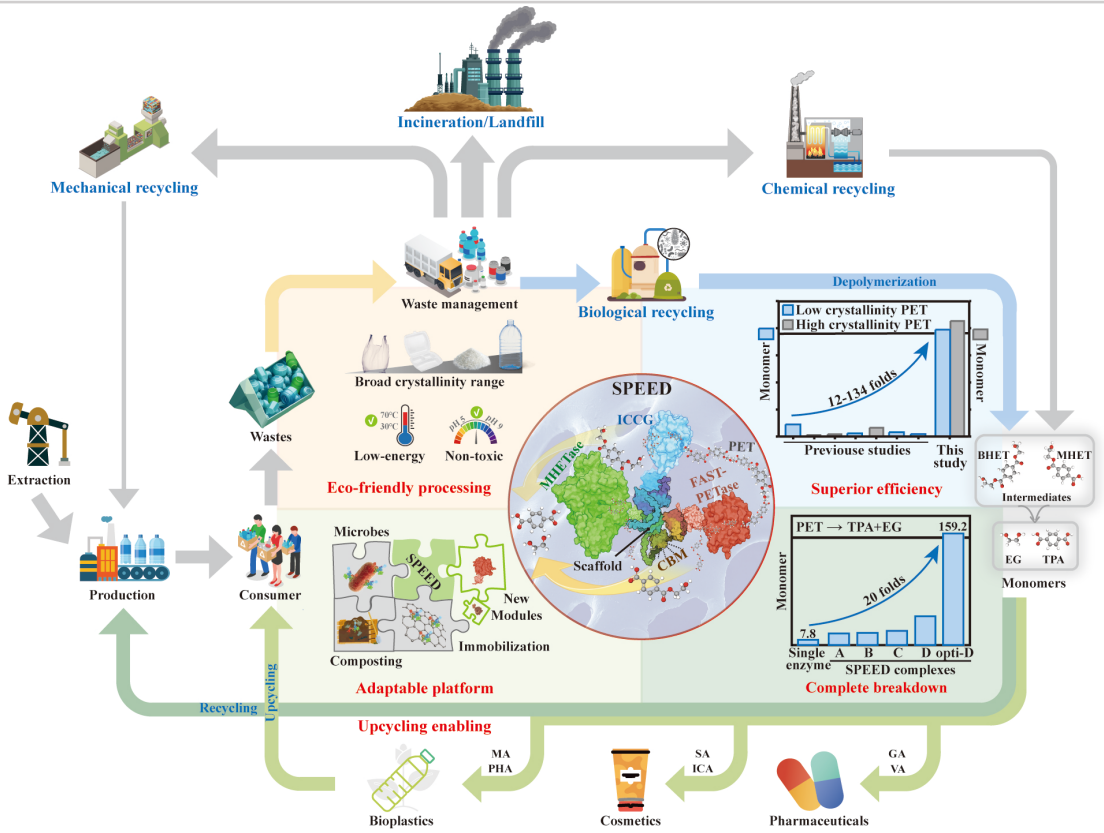

Fig. 1: Schematic overview of PET recycling pathways, highlighting SPEED's role in promoting a circular PET economy. Arrows depict the mechanical, chemical and biological PET recycling processes. The SPEED system (central circle) utilizes a modular enzyme-scaffold complex to achieve complete depolymerization of various PET substrates with a broad range of crystallinity into valuable monomers, terephthalate (TPA) and ethylene glycol (EG). Key advantages of SPEED at different stages of the recycling and upcycling processes are highlighted. The enzyme-scaffold complex structure was constructed by integrating PETase structures from the PDB with an AlphaFold2-predicted scaffold model. Abbreviations: MA, *cis*-muconic acid; PHA, polyhydroxyalkanoate; SA, succinic acid; ICA, isocinchomeronic acid; GA, gallic acid; VA, vanillic acid.

67 **Table 1. Current multi-enzyme systems for biodegradation of PET plastics**

System	PET substrate*	Reaction condition	Enzymes	Total products (mM)	Reaction volume (mL)	Degradation efficiency (mol total products /mmol enzyme)	Efficiency fold-change (SPEED vs. other systems)	Reference
HiC+CALB	Bottle-H	60°C, 14 days, pH 7	225 nmol HiC + 24.24 nmol CALB	2.247	5	0.045	133.8 (SPEED★)	19
HiC+CALB	Bottle-H	60°C, 14 days, pH 7	62.5 nmol HiC + 60.61 nmol CALB	0.728	10	0.06	102.0 (SPEED★)	20
TfCa+LCC	Film-L	60°C, 24 h, pH 9	21.7 nmol TfCa (immobilized) + 13.85 nmol LCC	10.42 (TPA: 6.71, M/BHET: 3.71)	40	11.72	4.7 (total) 13.0 (TPA) (SPEED♠)	22
PETase+ MHETase	Film-L	30°C, 96 h, pH 7.5	0.33 nmol PETase + 0.081 nmol MHETase	2.87	0.5	3.47	28.6 (SPEED♣)	21
cPETase+ cCALB+ mCbpA (scaffold)	Waste-H	30°C, 96 h pH 7	10 nmol cPETase + 10 nmol cCALB	0.04	40+	0.08	26.9 (SPEED♦)	25
	Film-H			0.089		0.18	12.1 (SPEED♦)	
LCC+TTCE	Film-L	60°C, 96 h, pH 8	1 nmol LCC + 1 nmol TTCE	17.97	0.5	4.49	22.1 (SPEED♣)	23
TfCaWA+ *Is*PETasePM	Film-L	45°C, 24 h, pH 7.5	0.05 nmol PETase + 0.55 nmol TfCa	1.68	1	2.80	19.7 (SPEED♠)	24
SPEED (FAST-PETase+ MHETase+ ICCG+Scaffold)	Film-L	40°C, 24 h, pH 7	0.25 nmol FAST + 0.25 nmol MHETase + 0.25 nmol ICCG	82.87	0.5	55.25 (♠)	-	This study (**Fig. 5**)
	Powder-H	40°C, 96 h, pH 7		143.76		95.84 (♥)	-	
	Film-L			148.82		99.21 (♣)	-	
	Film-H			3.23		2.15 (♦)	-	
	Film-L	40°C, 14 days, pH 7		189.85		126.57 (■)	-	
	Film-H			9.05		6.03 (★)	-	

68 Note: **a.** * Substrates can vary in different studies. To facilitate their comparison, we define substrates as follows: L:
69 low crystallinity (< 20%), H: high crystallinity (> 20%). **b.** + Where reaction volume was not specified in the original
70 publication nor provided by the corresponding author, a reaction volume of 40 mL was assumed for efficiency
71 calculations, based on the largest volume reported in similar studies listed in Table 1. **c.** Total products include TPA,
72 MHET, and BHET. **d.** Extended details associated of this table is provided in **Supplementary File 1**.

Results

Synergistic enzyme-scaffold system for enhanced PET degradation

To harness the complementary properties of different PET hydrolases and promote their synergy, we utilized the established dockerin-cohesin (doc-coh) pairs [26] to assemble multiple PET hydrolases onto a tailored scaffold. We initially selected FAST-PETase [15], for its potent PET hydrolysis at ambient conditions, and MHETase [13] for its ability to convert hydrolysis intermediates bis-(2-hydroxyethyl) terephthalate (BHET) and mono-(2-hydroxyethyl) terephthalate (MHET) into valuable monomers terephthalic acid (TPA) and ethylene glycol (EG) (**Fig. 2a**).

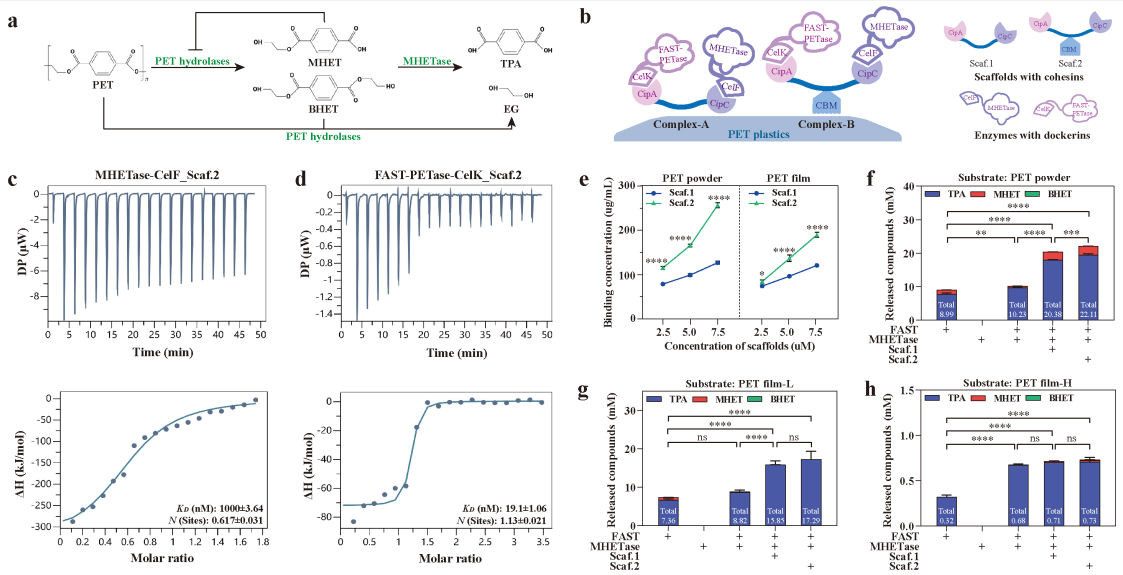

Fig. 2: Enzyme-scaffold complexes enhance PET degradation efficiency. a Schematic of enzymatic PET hydrolysis. Hydrolysis intermediates MHET and BHET can inhibit PETase activity, which is mitigated by MHETase. **b** Schematic of enzyme-scaffold complexes. Enzymes with complementary PET degradation activities are fused with dockerin domains, enabling co-assembly with a cohesin-containing scaffold. **c-d** Binding analysis of MHETase-CelF **(c)** and FAST-PETase-CelK **(d)** to Scaf.2 (CipA-CBM-CipC). **e** Binding affinity of scaffolds to PET substrates. **f-h** PET degradation assays comparing various enzyme and scaffold combinations on different substrates: PET powder (40.8% crystallinity) **(f)**, low crystallinity PET film (film-L, 18.0% crystallinity) **(g)**, and high crystallinity PET film (film-H, 43.3% crystallinity) **(h)**; reactions were performed at 30°C, pH 7.0, for 96 hours using 100 mg PET substrate, 0.2 nmol individual enzymes, with an enzyme:scaffold molar ratio of 0.2:1. Data are presented as mean ± s.d. (n = 3). Statistical significance was determined by one-way ANOVA (ns: not significant, *p < 0.1, **p < 0.01, ***p < 0.001, ****p < 0.0001).

PET biodegradation assays confirmed the synergistic effects of FAST and MHETase in hydrolyzing PET with different crystallinity (**Fig. 2f-h** and **Supplementary Fig. 3**). Consistent with previous findings [13], FAST alone readily hydrolyzed PET, while MHETase exhibited no independent activity. While combining these enzymes enhanced degradation, particularly for high-crystallinity substrates, further improvements were achieved by assembling them onto Scaf.1 (Complex-A). This resulted in over two-fold increases in total PET hydrolysis compared to FAST alone for all tested substrates, and a two-fold increase for PET powder and low-crystallinity film (film-L) compared to

102 the enzyme mixture without scaffold. Notably, complexes with Scaf.2 (Complex-B) slightly
103 outperformed those with Scaf.1, yielding 22.11 mM (PET powder), 17.29 mM (film-L), and 0.73
104 mM (film-H) total products after 96 hours.

105 **Optimization of MHETase expression, assembly, and activity**

106 The above results highlight the importance of MHETase in mitigating the competitive inhibition of
107 intermediates to PET hydrolases (**Fig. 2a**). However, the extremely low expression level of
108 recombinant MHETase in *E.coli*, hindered our further development (**Supplementary Fig. 4a**,**b**). To
109 address this bottleneck, we pursued a multi-pronged optimization strategy focusing on host strain
110 selection, induction conditions, codon usage, and protein domain fusions (**Fig. 3a**,**b** and
111 **Supplementary Fig. 4**,**5**). This led to the creation of $SH3_L$-optiMHETase and a redesigned scaffold,
112 CipA-CBM-$SH3_D$ (Scaf.3). Importantly, $SH3_L$-optiMHETase demonstrated significantly improved
113 binding affinity to Scaf.3 (an 80-fold enhancement compared to MHETase-CelF (**Fig. 3c** vs. **Fig.**
114 **2c**), reaching a level comparable to FAST (**Fig. 3c-e**). These modifications enabled the successful
115 assembly of Complex-C (**Fig. 3a**).

116 Degradation assays across various PET substrates revealed significant improvements (**Fig. 3f-**
117 **h**). Complex-C yielded 22.37 mM, 23.22 mM and 0.83 mM TPA production with PET powder, film-
118 L and film-H, respectively. This represents a 3-fold increase over FAST-only groups and a 22.2%
119 average increase over Complex-B (**Fig. 3f-h** vs. **Fig. 2f-h**). These results confirm Complex-C's
120 effectiveness in promoting PET recycling, highlighting SPEED's adaptability and potential for cost
121 reduction in complex construction.

122 **Modular scaffold expansion to boost PET degradation capacity**

123 Our optimization from Complex-A to Complex-C exemplifies the power of SPEED's modular
124 scaffold design, allowing for tailored enzyme combinations for diverse substrates. To broaden
125 substrate range, we incorporated ICCG, an enzyme active towards higher-crystallinity substrates
126 (6%-40%) [27], complementing the preference of FAST-PETase for lower-crystallinity PET (1%-30%)
127 [15]. Using the doc-coh pair ScaA-ScaB [28] we successfully integrated ICCG into a new scaffold, CipA-
128 CBM-$SH3_D$-ScaB (Scaf.4), forming Complex-D (**Fig. 4a** and **Supplementary Fig. 6**).

129 Degradation assays revealed several key insights (**Fig. 4b-d**). The result showed ICCG has
130 slightly higher activity towards PET substrates compared to FAST at 30°C. Notably, inclusion of
131 MHETase with ICCG led to near-complete conversion of MHET and BHET intermediates into TPA,
132 and EG by implication. Moreover, combining ICCG, FAST, and MHETase greatly increased TPA
133 productions to 33.07 mM (powder), 36.09 mM (film-L) and 0.93 mM (film-H). Importantly, Scaf.4
134 further boosted the efficiency to 44.66 mM (powder), 49.03 mM (film-L) and 1.32 mM (film-H).
135 Finally, we confirmed the strong binding of all three enzymes (FAST, MHETase, and ICCG) to the
136 scaffold, demonstrating stability of Complex-D (**Fig. 4e-g**). Overall, Complex-D further enhanced
137 PET biodegradation efficiency and achieved complete monomer conversion.

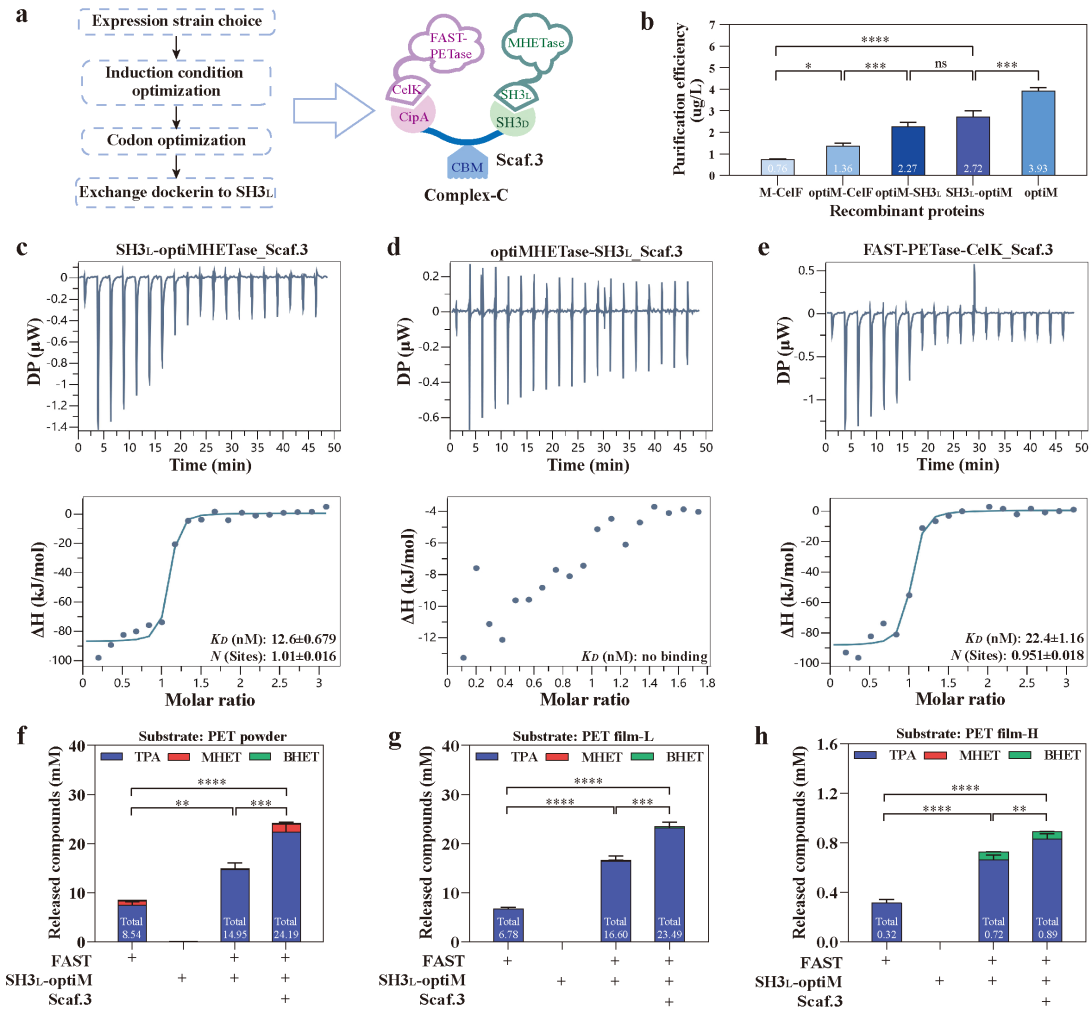

Fig. 3: MHETase optimization for enhanced expression, scaffold binding, and PET degradation. a Schematic illustration of MHETase optimization strategy and the assembly of Complex-C with Scaf.3 (CipA-CBM-SH3D). **b** Purification efficiency of different MHETase variants. M-CelF: MHETase-CelF; optiM-CelF: codon optimized M-CelF; M-optiSH3L: optiMHETase-SH3L; SH3L-optiM: SH3L-optiMHETase; optiM: codon optimized MHETase (as control); **c-e** Binding analysis of SH3L-optiMHETase **(c)**, optiMHETase-SH3L **(d)**, and FAST-PETase-CelK **(e)** to Scaf.3. **f-h** PET degradation assays using FAST and SH3L-optiM, assembled with Scaf.3, on various substrates: PET powder **(f)**, film-L **(g)**, and film-H **(h)**. All reactions were performed at 30°C, pH 7.0, for 96 hours using 100 mg PET substrate, with an enzyme:scaffold molar ratio of 0.2:1. Data are presented as mean ± s.d. (n = 3). Statistical significance was determined by one-way ANOVA (ns: not significant, *p < 0.1, **p < 0.01, ***p < 0.001, ****p < 0.0001).

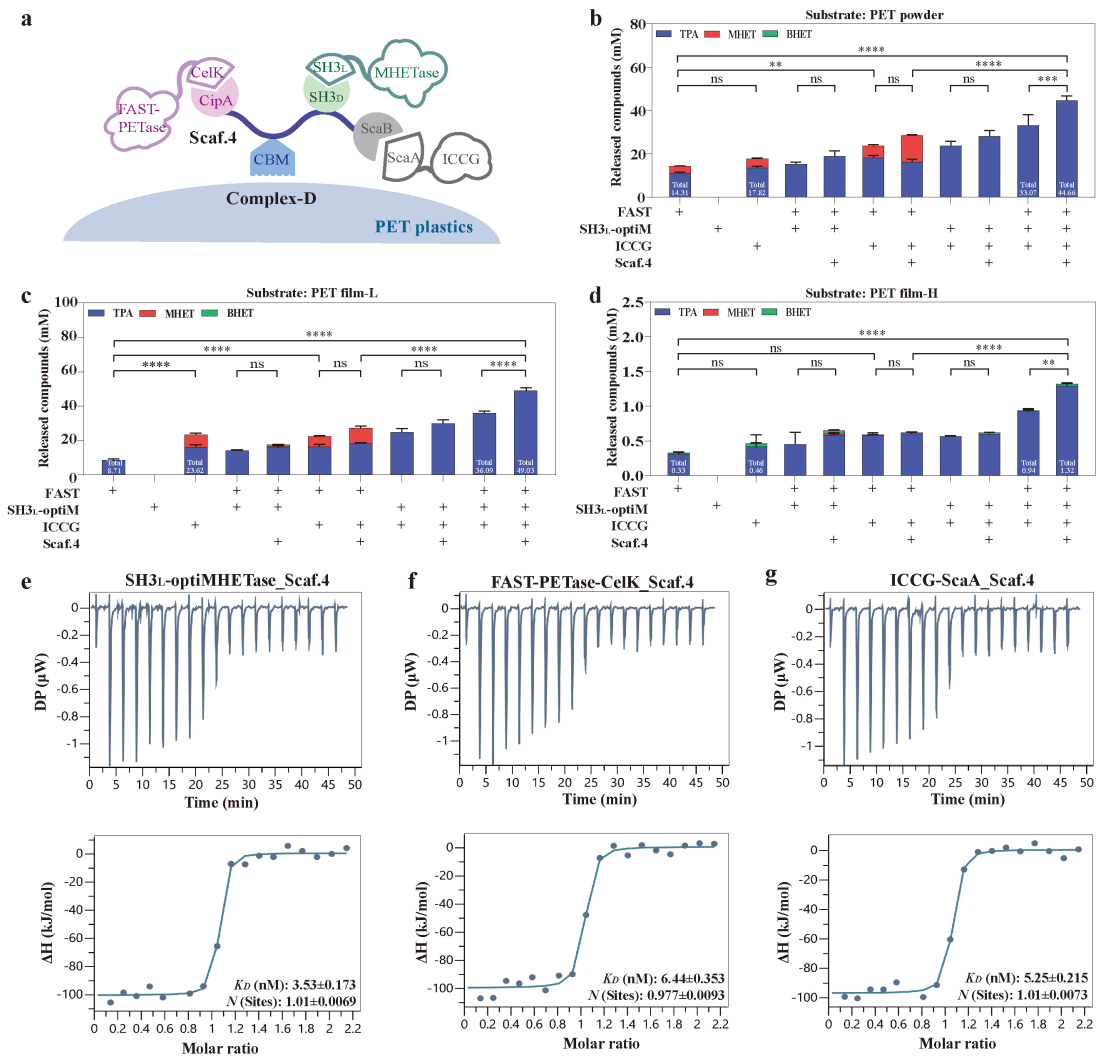

Fig. 4: Scaffold engineering further enhances PET degradation with a three-enzyme complex. a Schematic illustration of Complex-D, formed by the assembly of three hydrolases (FAST-CelK, $SH3_L$-optiMHETase, ICCG-ScaA) onto the modular scaffold Scaf.4 (CipA-CBM-$SH3_D$-ScaB). **b-d** PET degradation assays comparing the activity of individual hydrolases and Complex-D on different substrates: PET powder **(b)**, film-L **(c)**, and film-H **(d)**. All reactions were performed at 30°C, pH 7.0, for 96 hours using 100 mg PET substrate, with an enzyme:scaffold molar ratio of 0.2:1. Data are presented as mean ± s.d. (n = 3). Statistical significance was determined by one-way ANOVA (ns: not significant, *p < 0.1, **p < 0.01, ***p < 0.001, ****p < 0.0001). **e-g,** Binding analysis of $SH3_L$-optiMHETase **(e)**, FAST-CelK **(f)**, and ICCG-ScaA **(g)** to Scaf.4.

Improve SPEED performance through reaction optimization

To optimize the performance of the three-enzyme Complex-D and improve enzyme cost-effectiveness, we systematically investigated its PET degradation efficiency under various reaction conditions (**Fig. 5a**), beginning with the impact of enzyme-scaffold ratio (**Fig. 5b**). While increasing enzyme concentration enhanced product release (**Fig. 5b**, bar graph), ratios exceeding 0.5:1 (enzyme:Scaf.4) led to diminishing benefits from the scaffold (**Fig. 5b**, dot graph and **Supplementary Fig. 7**). This suggests that excessive enzymes may not only increase costs but also hinder substrate channeling due to limited scaffold availability. Consequently, we adopted the 0.5:1

166 enzyme-to-scaffold ratio for subsequent optimizations.

167 Next, we investigated the influence of temperature and PH on Complex-D performance (**Fig.**
168 **5c**,**d**). According to previous findings [29], the optimal temperatures for FAST and ICCG were
169 approximately 40°C and 60°C, respectively. Our results showed that further temperature increases
170 above 40°C resulted in elevated levels of intermediates and reduced TPA production, likely due to
171 adverse effects on enzyme activity of MHETase (**Supplementary Fig. 8**). The highest total product
172 yield (176.40 mM with 174.71 mM TPA) was achieved at 40°C and pH 7.0, which consists with the
173 optimal conditions for MHETase activity [30]. Next, the robustness of Complex-D under these optimal
174 conditions was validated across diverse PET substrates, including PET powder, films and
175 commercial bottles, confirming its outstanding ability to mediate complete PET degradation
176 (**Supplementary Fig. 9**).

177 The catalytic stability and substrate versatility of Complex-D, were assessed through long-term
178 PET degradation experiments under optimal conditions (40°C, pH 7.0, 0.5:1 Enz.:Scaf. ratio). This
179 complex exhibited robust and sustained hydrolysis across diverse PET substrates (**Fig. 5e-g**).
180 Scanning electron microscopy (SEM) revealed that treatment with the optimized Complex-D
181 (optiComplexD) induced significantly greater surface erosion and pore formation on PET film after
182 96 hours, compared to individual enzymes (FAST, ICCG, or MHETase) (**Fig. 5h**).

183 **MOF immobilization enhances SPEED performance and reusability**

184 To enhance the system's stability and reusability for industrial translation, we immobilized
185 optiComplex-D onto the metal-organic framework ZIF-8 [31] (**Fig. 6a**). The successful synthesis of
186 enzyme complex-conjugated ZIF-8 (optiComplex-D@ZIF-8) was characterized by SEM,
187 fluorescent microscopy, and further confirmed by XRD analysis, which showed strong peaks
188 matching the simulated ZIF-8 with a high loading efficiency of 92.8% (**Fig. 6a**,**b** and
189 **Supplementary Fig. 10**). Indeed, MOF immobilization further enhanced PET biocatalysis (**Fig.**
190 **6d**). Notably, optiComplex-D@ZIF-8 exhibited a 151% increase in PET degradation efficiency
191 compared to the enzyme mixture without the scaffold (Enz.3@ZIF-8), underscoring the importance
192 of the scaffold design even after the immobilization. Furthermore, immobilization significantly
193 improved the complex's stability across a wider pH range, with optiComplex-D@ZIF-8 showing
194 2.1-fold and 1.6-fold higher activity at pH 5.0 and 9.0, respectively, compared to the free
195 optiComplex-D (**Fig. 6e**). The reusability of optiComplex-D@ZIF-8 was also remarkable, retaining
196 52.2% activity after four 4-day cycles, significantly surpassing the 24.4% retained activity of
197 optiComplex-D without immobilization (**Fig. 6f**). Critically, the inclusion of the nano-scaffold
198 remained crucial even after ZIF-8 immobilization, as it exhibited superior long-term degradation
199 activity (**Fig. 6g**). This enhanced stability and reusability, coupled with the superior degradation
200 efficiency, underscore the potential of SPEED for cost-effective and sustainable PET recycling by
201 reducing enzyme consumption and improving process efficiency.

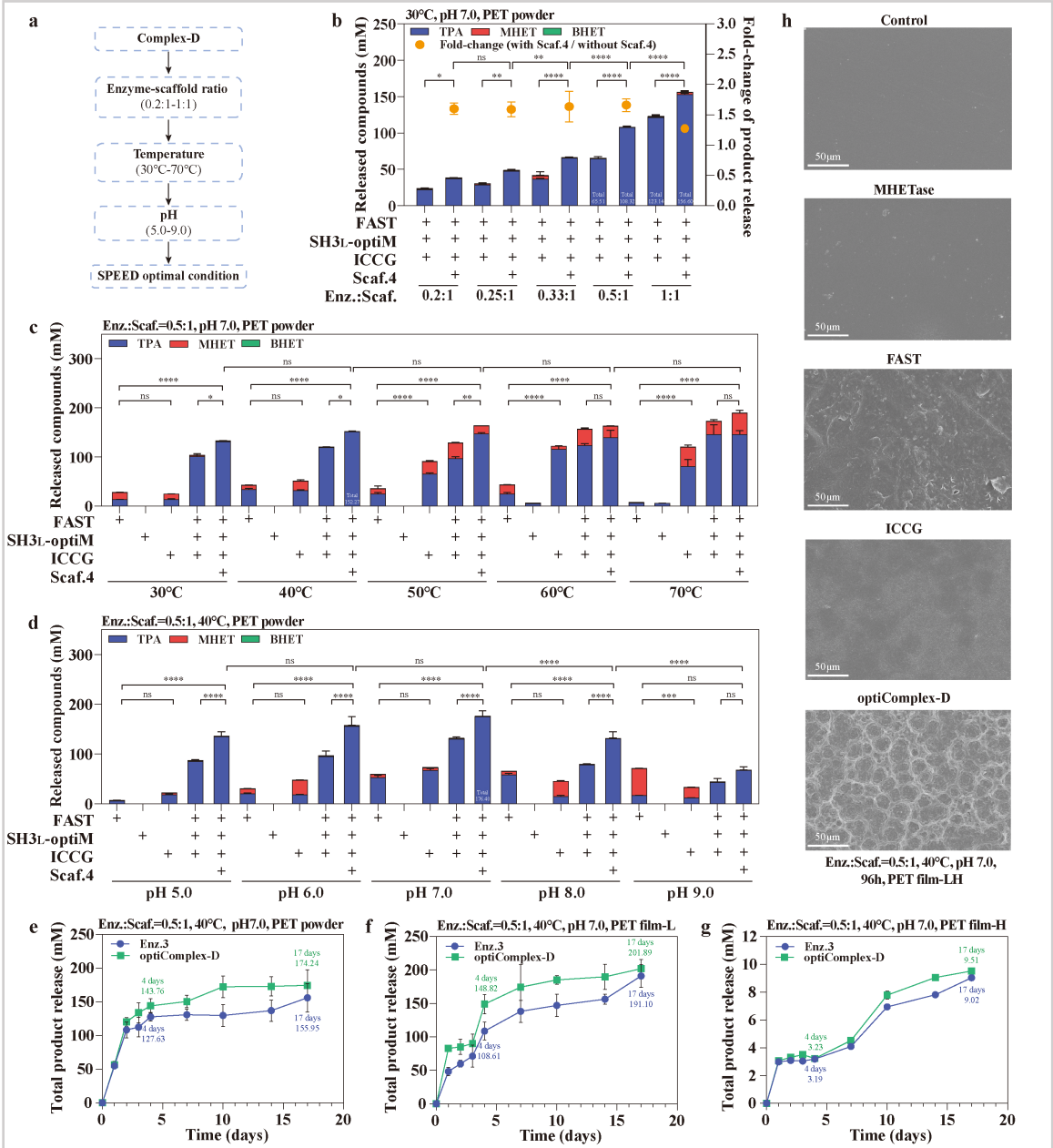

Fig. 5: Optimization of SPEED reaction conditions. a Overview of the optimization strategy. **b** Effect of enzyme-to-scaffold molar ratio on PET degradation efficiency (30°C, pH 7.0, 96 hours, 100 mg PET powder, with a constant 1 mM scaffold concentration). Total product release (bar graph, left Y axis) and fold-change in efficiency with vs. without Scaf.4 (dot graph, right Y axis) are shown. **c** Influence of temperature on PET degradation efficiency and final products (0.5:1 enzyme:scaffold ratio, pH 7.0, 96 hours, 100 mg PET powder). **d** Impact of pH on PET degradation efficiency and final products (0.5:1 enzyme:scaffold ratio, 40°C, 96 hours, 100 mg PET powder). **e-g** Time-course analysis of PET degradation by optiComplex-D (40°C, pH 7.0, 0.5:1 enzyme:scaffold ratio) on different substrates**:** PET powder **(e),** film-L **(f)**, and film-H **(g)**. **h** SEM images of film-L after 96 hours of treatment at 40°C, pH 7.0, with no enzyme (Control), single enzyme (MHETase, FAST, ICCG), and optiComplex-D. Data are presented as mean ± s.d. (n = 3). Statistical significance was determined by one-way ANOVA (ns: not significant, *p < 0.1, **p < 0.01, ***p < 0.001, ****p < 0.0001).

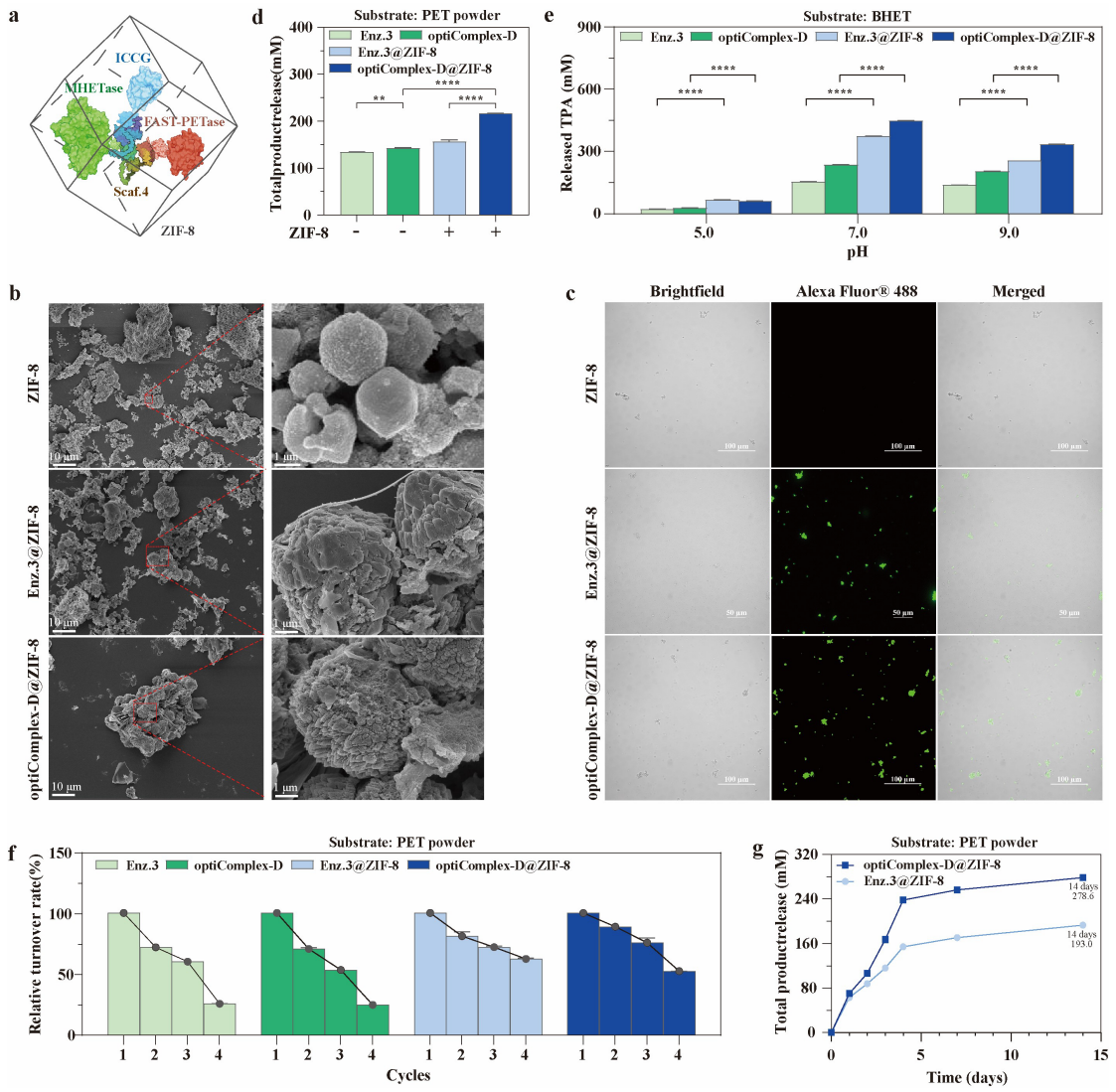

Fig. 6: MOF immobilization enhances SPEED performance and reusability. a Schematic illustration of optiComplex-D immobilized on ZIF-8 (optiComplex-D@ZIF-8). **b** SEM images of ZIF-8, Enz.3@ZIF-8 and optiComplex-D@ZIF-8. **c** Confocal microscope images of ZIF-8, Enz.3@ZIF-8 and optiComplex-D@ZIF-8. Alexa Fluor® 488 was used to detect His-tagged proteins. **d** PET degradation assays with PET powder at 40°C, pH 7.0, for 96 hours. **e** Impact of pH on TPA release at 40°C for 96 hours, with 1 M BHET as substrate. **f** Relative PET catalysis activity in each of the 4-day cycles normalized to the initial cycle. **g** Time-course analysis of PET degradation at 40°C, pH 7.0, with 0.5:1 enzyme:scaffold ratio on PET powder. Enz.3 represents a mixture of FAST-PETase, ICCG, and MHETase (0.25 nmol of each enzyme). Data are presented as mean ± s.d. (n = 3). Statistical significance was determined by one-way ANOVA (ns: not significant, *p < 0.1, **p < 0.01, ***p < 0.001, ****p < 0.0001).

PET upcycling through SPEED-enabled biocatalysis

The efficient depolymerization of PET by optiComplex-D provides an opportunity for coupling the upcycling of the resulting monomers into high-value chemicals [32–34]. To showcase this capability, we leveraged the SPEED platform's modularity to engineer a multi-enzyme assembly (Complex-E) capable of converting PET degradation product ethylene glycol (EG) to gallic acid (GA), a valuable compound with applications in in inflammation treatment and pathogen resistance [35–37]. The

conversion pathway we designed involves the sequential action of 1,2-propanediol oxidoreductase (FucO) [38] and glycolaldehyde dehydrogenase (AldA) [39], with *Lactobacillus reuteri* NADH oxidase (LrNox) [40] regenerating the required NAD^+ cofactor, a similar strategy builds upon our prior work (**Fig. 7a**,**b**).

We explored two reaction designs to evaluate GA production efficiency. First, adding Complex-E to the PET degradation products generated by Complex-D resulted in 2.65 mM GA in 4 days (**Fig. 7c**). Next, simultaneous addition of Complex-D and E further promoted GA production to 4.61 mM in 4 days, a 1.74-fold increase (**Fig. 7d**), which likely stems from the synergistic action of both complexes, enabling real-time conversion of the intermediate EG. Interestingly, the simultaneous addition of free upcycling enzymes initially reduced Complex-D's PET degradation rate (**Fig. 7e**), likely due their competition for Scaf.4 binding sites. However, pre-incubating the upcycling enzymes with Scaf.4 before adding to Complex-D eliminated this competition, highlighting the scaffold's ability to promote synergistic interactions while preventing interference between different enzyme complexes.

Overall, the successful upcycling of PET waste into GA showcases the SPEED platform's effectiveness in assembling diverse enzymes, improving reaction efficiency, and enabling a promising strategy for multi-enzyme biocatalysis towards a circular PET economy.

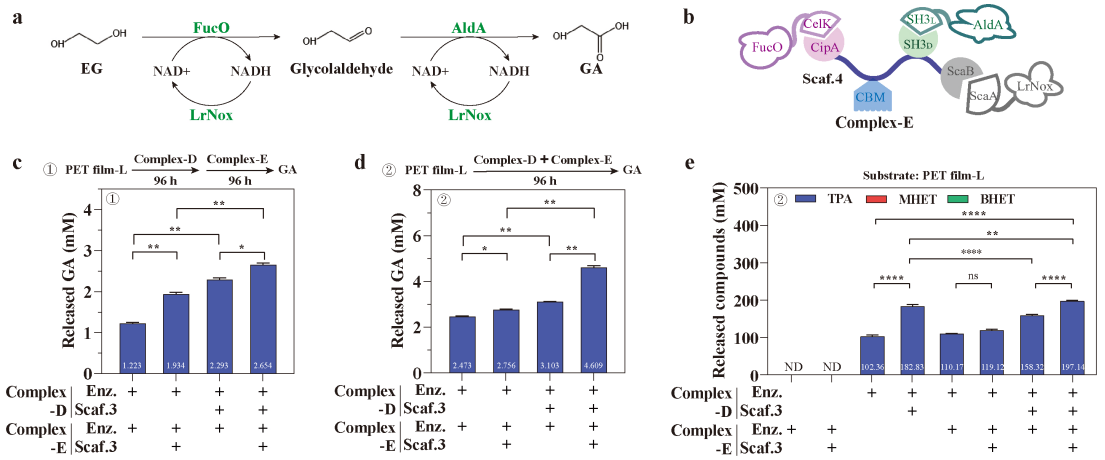

Fig. 7: Valorization of PET waste via SPEED-enabled upcycling. a Schematic of the enzymatic synthesis pathway for gallic acid (GA). **b** Schematic illustration of Complex-E. **c-d** GA production assays after 4-day, , using either sequential addition of Complex-D (for PET degradation) followed by Complex-E (for GA production) **(c)** or simultaneous addition of both complexes to the PET substrate **(d)**. **e** PET degradation performance under different enzyme and scaffold combinations. All reactions were performed at 40°C, pH 7.0, for 96 hours, with 0.5 nmol of each individual enzyme and enzyme:scaffold molar ratios of 0.5:1 for optiComplex-D and 1:1 for Complex-E. ND, not detected. Data are presented as mean ± s.d. (n = 3). Statistical significance was determined by one-way ANOVA (ns: not significant, *p < 0.1, **p < 0.01, ***p < 0.001, ****p < 0.0001).

Cell surface display expands SPEED to live cell systems

To further demonstrate the adaptability of SPEED for industrial PET biorecycling, we explored its integration with cell surface display technology, aiming to create a cost-effective live cell system compatible with large-scale fermentation processes [41]. We selected the industrial yeast *Pichia pastoris* for its ability to achieve high-yield protein production, attributed to its high growth density and secretion capacity [42,43]. Among various *P. pastoris* strains, we chose the SMD1168 strain for its superior capacity to display the scaffold on the cell surface and secrete PETases (**Fig. 8a** and **Supplementary Fig. 11**). The scaffold expressed by the engineered strain was displayed to the cell surface using the SED1 protein, which demonstrated the highest efficiency among the tested anchors (**Fig. 8b**). Confocal microscopy and flow cytometry confirmed the successful assembly of the multi-enzyme complex on the engineered *P. pastoris* cell surface (**Fig. 8c**,**d**). The surface-displayed SPEED Complex-B, facilitated by the scaffold, exhibited a remarkable increase in PET degradation efficiency, up to 3.05-fold higher than the secreted enzyme group [42,43] (**Fig. 8e**). This result underscores the advantage of enzyme synergy enabled by our SPEED design in accelerating PET degradation, both *in vitro* and *in vivo*.

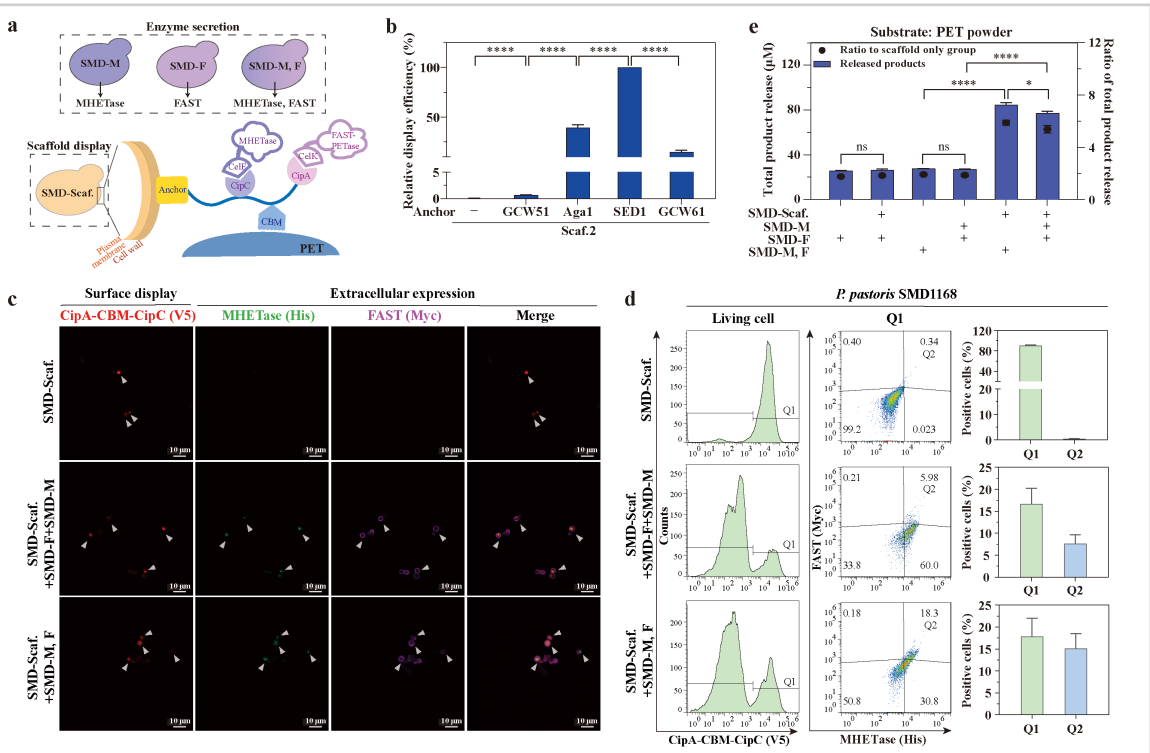

Fig. 8: SPEED-enabled live cell system for PET degradation. a Schematic of the engineered *P. pastoris* SMD1168 system for cell-surface display of the enzyme complex. **b** Cell surface display efficiency of the scaffold using different anchor proteins. The relative efficiency was calculated by taking the maximum display efficiency as 100%. NC, negative control (scaffold fused with no anchor). **c-d** Characterization of engineered strains by confocal microscopy **(c)** and flow cytometry **(d)**. **e** PET degradation assays using the engineered *P. pastoris* strains. Expression and reactions were performed at 30°C, pH 7.0, for 96 h (induction) and 48 h (reaction) with 100 mg PET powder substrate. The ratio of enzyme-secreting strains to the scaffold-displaying strain was 10:1. Statistical significance was determined by one-way ANOVA (ns: not significant, *p < 0.1, **p < 0.01, ***p < 0.001, ****p < 0.0001).

Discussion

Our study demonstrates SPEED's potential to transform current PET waste management. By achieving unprecedented efficiency across diverse PET waste substrates, SPEED offers significant advances over existing biocatalytic systems. This superior performance stems from several factors. The modular design of the nano-scaffold enables the integration of multiple enzymes with complementary activities, facilitating synergistic PET degradation and complete conversion to high-value monomers (TPA and EG). This complete depolymerization, evident in the minimal accumulation of intermediates, not only reduces environmental impact but also enhances the economic viability of biorecycling by generating products suitable for direct upcycling. Additionally, the strategic selection of enzymes with optimal activity at 40°C and pH 7.0, as well as the optimization of the enzyme-to-scaffold ratio, further contribute to SPEED's exceptional efficiency. These factors, along with the resolution of the MHETase expression and assembly bottleneck [44], collectively address the limitations of previous biocatalytic systems, such as incomplete conversion and intermediate inhibition, and pave the way for its industrial adoption.

Furthermore, SPEED's significant efficiency gains, the modular flexibility and the lower enzyme requirement for comparable performance highlight its cost-effectiveness. This addresses one of the major hurdles to large-scale adoption of biocatalytic PET recycling [29,45]. The modularity of SPEED also opens up opportunities for customization, potentially enabling the degradation of diverse PET waste streams with tailored enzyme cocktails.

Beyond its immediate impact on PET recycling, SPEED offers a broader contribution to sustainable materials management. The successful upcycling of PET waste into high-value compounds like gallic acid, exemplifies the platform's potential to drive a circular economy. Additionally, SPEED's compatibility with other strategies, such as cell surface display and enzyme immobilization, further enhances its efficiency and broadens its applicability. The SPEED-enabled live cell system offers additional benefits such as eliminating the need for antibiotics, ensuring stable enzyme production, and reducing plastic degradation costs. The integration of SPEED into existing industrial processes could reduce reliance on fossil fuels for PET production, while promoting circularity by closing the loop on plastic waste.

While our work demonstrates the promise of SPEED, challenges remain in scaling up the technology and ensuring its economic viability at an industrial level. Further research is needed to optimize enzyme production costs and explore the potential for incorporating additional upcycling enzymes [33]. Nevertheless, the results presented here underscore the transformative potential of nano-scaffolded enzyme complex platform such as SPEED in addressing the global plastic waste crisis and accelerating the transition towards a circular economy model. With its proven efficiency and promising scalability, SPEED has great potential to revolutionize waste management practices, reducing environmental harm and promoting a more sustainable future.

322 ## Methods

323 ### Plasmid construction

324 Genes encoding enzymes and scaffolds were obtained from commercial synthesis (Tsingke, China).
325 Standard cloning techniques were employed using *E. coli* DH5α. Briefly, FAST-PETase, ICCG,
326 FucO, AldA, LrNox and scaffold variants were cloned into pET28a vectors, while MHETase
327 constructs utilized pET28a and pColdII vectors. Synthesized genes and pET28a vectors were
328 digested with NdeI and XhoI (37°C, 1h), followed by T4 DNA ligase-mediated ligation (room
329 temperature, 2h). This generated plasmids pET28a-FAST-PETase-CelK, pET28a-MHETase-CelF,
330 pET28a-ICCG-ScaA, pET28a-FucO-CelF, pET28a-$SH3_L$-AldA, pET28a-LrNox-ScaA, pET28a-
331 CipA-CBM-CipC, pET28a-CipA-CBM-$SH3_D$, and pET28a-CipA-CBM-$SH3_D$-ScaB.
332 To construct the living cell PET degradation system, *Pichia pastoris* SMD1168 was employed.
333 The pPIC9K vector was utilized for the insertion and expression of MHETase, and Scaf.3. To
334 engineer strain with exogenous gene insertion, primer pairs pScf-F/pScf-R were employed to
335 amplify CipA-CBM-CipC-SED1, while primer pairs pF-F/pF-R and pM-F/pM-R were utilized to
336 amplify FAST and MHETase, respectively. Additionally, primers pPIC9K-F/pPIC9K-R was used
337 to amplify pPIC9K linearized vector. The pPICZC vector was utilized for the insertion of MHETase.
338 MHETase and pPICZC linearized vector were amplified using primer pairs pZM-F/pZM-R and
339 pPICZC-F/pPICZC-R. The linearized gene and vector were connected by seamless cloning to form
340 the expression vectors pPICZC-FAST, pPIC9K-MHETase, pPIC9K-CipA-CBM-CipC-SED1, and
341 pPICZC-MHETase. The expression vectors were linearized by SacI digestion and transformed into
342 *P. pastoris* SMD1168. The transformants were cultured in histidine-deficient (SD-his) plates and
343 screened for strains with high copies of the exogenous gene insertion by SD-his plates containing 5
344 mg/mL G418.
345 To reposition $SH3_L$ from the C-terminus to the N-terminus of optiMHETase, sequential PCR
346 was performed with primer pairs M1-F/M-R, M2-F/M-R, and M3-F/M-R. To remove $SH3_L$ from
347 $SH3_L$-optiMHETase (as control), PCR was performed with primer pairs M1-F/Md-R. For C-
348 terminal His-tag of MHETase, PCR was conducted using primers his-F/his-R. Subsequent digestion
349 with NdeI and XbaI, followed by T4 DNA ligase-mediated recombination, generated plasmids
350 pColdII-MHETase-CelF, pColdII-optiMHETase-CelF, pColdII-optiMHETase-$SH3_L$, pColdII-
351 $SH3_L$-optiMHETase, and pColdII-optiMHETase. All protein constructs were designed with both N-
352 and C-terminal His tags.

353 ### Exogenous gene insertion analysis

354 The insertion copy number of exogenous genes was determined by quantitative real-time PCR
355 (qPCR). The genomic DNA of engineered *P. pastoris* SMD1168 was extracted by the Yeast
356 Genomic DNA Extraction Kit (TIANGEN, DP307). Genomic DNA of *P. pastoris*
357 $SMD1168_{His4::CipA\text{-}CBM\text{-}CipC\text{-}SED1}$, *P. pastoris* $SMD1168_{His4::FAST}$, *P. pastoris* $SMD1168_{His4::MHETase}$
358 and *P. pastoris* $SMD1168_{His4::FAST\text{-}MHETase}$ were used as templates, respectively, for the amplification

359 of the genes CipA-CBM-CipC, FAST, MHETase with the primer pairs qC-F/qC-R, qF-F/qF-R, and
360 qM-F/qM-R; the housekeeping gene GAPDH was amplified with the primer pairs qGAPDH-
361 F/qGAPDH-R to obtain the copy number of the exogenous protein inserted in the engineered strains.

362 **Recombinant protein expression and purification**

363 For living cell systems, surface-displaying and secretory-expressing engineered bacteria were
364 individually pre-cultured in BMGY (1% yeast extract, 2% peptone, 100 mM potassium phosphate
365 buffer, 1.34% amino acid-free yeast nitrogen source, and 1% (v/v) glycerol, pH 6.0) at 30°C for 12
366 h, after which the number of cells was measured in the pre-cultured products. *P. pastoris*
367 SMD1168$_{His4::enzyme}$ was mixed with *P. pastoris* SMD1168$_{His4::scaffold}$ in a 10:1 ratio, resulting in a
368 final system comprising 2×10^7 *P. pastoris* SMD1168$_{His4::scaffold}$. The expression medium BMMY (1%
369 yeast extract, 2% peptone, 100 mM potassium phosphate buffer, 1.34% amino acid-free yeast
370 nitrogen, and 1% (v/v) methanol, pH 6.0) was employed for protein expression and enzyme-scaffold
371 assembly. Expression was conducted at 30°C, with the medium augmented with 0.5% methanol at
372 24-hour intervals over a period of 96 hours.

373 For in vitro protein expression, *E. coli* C41 (DE3) cells were transformed with pColdII-based
374 plasmids, while *E. coli* BL21 (DE3) and *E. coli* Rosetta (DE3) cells were used for pET28a constructs.
375 Transformants were grown in LB media supplemented with appropriate antibiotics (100 μg/mL
376 ampicillin for pColdII, 500 μg/mL kanamycin for pET28a) at 37°C until OD_{600} reached 0.6-0.7.
377 IPTG (0.5 mM or 1.0 mM final concentration for MHETases, 1.0 mM for others) induced expression
378 overnight (at 16°C or 37°C for MHETases, 16°C for others). Cells were harvested by centrifugation
379 and stored at -80°C.

380 Cells were resuspended in lysis buffer (50 mM sodium phosphate, 300 mM NaCl, pH 8.0),
381 disrupted by sonication, and the supernatant was collected by centrifugation. HisTrap HP column
382 purification employed an ÄKTA pure system (Cytiva, China). Bound protein was washed with 85%
383 binding buffer (20 mM sodium phosphate, 30 mM imidazole, 500 mM NaCl, pH 7.4) with 15%
384 elution buffer (20 mM sodium phosphate, 500 mM imidazole, 500 mM NaCl, pH 7.4) and eluted
385 with a linear gradient of 15-100% elution buffer. Eluates were concentrated (Amicon Ultra, Merck
386 Millipore, China), buffer-exchanged to 50 mM sodium phosphate (SP buffer, pH 7.0), and assessed
387 for purity/concentration by NanoDrop™ One/One^C (Thermo Fisher, U.S.A.). Proteins were stored
388 in storage buffer (50% glycerol in SP buffer, pH 7.0) at -80°C.

389 **Binding assay of scaffold protein to PET**

390 Following previously established protocols [25], PET powder (crystalline, Xing-xiang new materials,
391 China) or PET film (amorphous, Goodfellow, UK) were washed with 10% SDS, water, and SP
392 buffer (pH 7.0). CipA-CipC (Scaf.1) or CipA-CBM-CipC (Scaf.2) were incubated at 2.5, 5, and 7.5
393 μM with 100 mg PET powder in 200 μL SP buffer (pH 7.0) overnight at 4°C. Samples were
394 centrifuged (12000 g, 1 min), washed twice with SP buffer (pH 7.0), and residual protein in solution
395 was quantified using a BCA Protein Quantification Kit (Yeason, China). Binding protein

concentration was calculated as follows (C, concentration; before, before incubation with PET; after, after incubation with PET):

$$Binding\ protein\ concentration = C_{(before)} - C_{(after)}$$

Binding assay of enzymes to scaffolds

Enzyme-scaffold protein interactions were analyzed by MicroCal PEAQ-ITC Automated (Malvern Panalytical, Netherland). Enzymes were placed in the reaction cell, and scaffold protein titrations were performed at 25°C with 18 injections of 2 μL substrate (details in Fig. legends). Dilution heats were corrected, and data were analyzed using the MicroCal PEAQ-ITC Analysis Software (one set of sites model).

For living cell system, flow cytometry was used to analyze enzyme-scaffold protein interactions. After a 96-hour induction at 30°C, the yeast cells were collected by centrifugation at 4000 g for 10 min at 4°C, then washed and diluted with DPBS. Subsequently, 1×10^7 cells and 0.1 μL of each antibody (V5 tag antibody, Invitrogen 451098; His tag antibody, Cell Signaling Technology 14930; or Myc tag antibody, R&D Systems IC3696P) were incubated (for 45 min) washed, and detected through flow cytometry.

Characterization of crystallinity of PET substrates

Thermal crystallinity of PET substates was determined by differential scanning calorimetry (DSC 8000, PerkinElmer). PET substrates (75 μm powder; low crystallinity PET film, film-L; high crystallinity PET film, film-H; Nongfu Spring water bottle, NFbottle) were heated from 30°C to 300°C at a heating rate of 30°C/min, kept at 300°C for 1 min, and then cooled to 0°C at 5 min with same rate of 30°C/min. The theoretical heat of melting value (ΔHm°) of 100% crystallized PET was 140.1 J/g. Percentage crystallinity was calculated with the heat of melting (ΔHm) and cold crystallization (ΔHc) values, as the following equation:

$$Crystallinity\ (\%) = \frac{\Delta Hm - \Delta Hc}{\Delta \mathrm{Hm}^\circ} \times 100\%$$

Synthesis and characterization of MOF-immobilized enzyme complexes

For synthesis of Complex-D@ZIF-8 and Enz.3@ZIF-8, 1.75 mL of 2-methylimidazole (2-MI, 790 mM), a certain amount of proteins (0.25 nmol individual enzyme of FAST, MHETase and ICCG with/without scaffold to form Complex-D/Enz.3), and 0.25 mL $Zn(NO_3)_2{\cdot}6H_2O$ (97.5 mM) was stirred at 500 g for 5 min. To synthesize ZIF-8, the same volume of 2-MI and $Zn(NO_3)_2{\cdot}6H_2O$ was stirred. Subsequently, the mixture was left undisturbed for 3 h at 4°C. Finally, the prepared Complex-D@ZIF-8, Enz.3@ZIF-8 and ZIF-8 were collected by centrifugation at 3500 g for 10 minutes and dispersed into 0.5 mL SP buffer.

For characterizations, confocal microscopy images were recorded by Nikon confocal laser scanning microscope with his-tag antibody (14930, Cell signaling technology); XRD (Bruker D8

430 Advance) and SEM (ZEISS GeminiSEM 300) were used to measure the immobilized samples.

431 **Characterization of living cell PET biodegradation systems**

432 Confocal microscopy images and flow cytometry assays were recorded by Nikon confocal laser
433 scanning microscope His Tag Alexa Fluor® 488-conjugated Antibody (IC0501G, R&D Systems),
434 V5 Tag Monoclonal Antibody (451098, Invitrogen), Human c-Myc PE-conjugated Antibody
435 (IC3696P, R&D Systems) to detect MHETase and/or FAST with his tag, FAST with myc tag,
436 scaffold with V5 tag, separately.

437 For surface displaying assays mediated by different anchors, displaying efficiency was
438 calculated with median florescence intensity (MFI) and copy number by flow cytometry and qPCR,
439 as the following equation:

440 $$Relative\ display\ efficiency = \frac{MFI_{V5\ positive}}{Copy\ number\ of\ the\ scaffold}$$

441 **Degradation assay of PET plastics**

442 Standard reactions contained 100 mg PET (powder, low or high crystallinity PET films), 0.2 mM
443 enzyme, 500 μL reaction buffer (50 mM sodium phosphate, 0.5 mM $CaCl_2$, 10% DMSO, pH 7.0).
444 For complex assembly, enzymes (0.2 mM) were pre-mixed with scaffold (1 mM) for 40 min at room
445 temperature. Unless otherwise stated, degradations proceeded for 96 h at 30°C.

446 To optimize the enzyme:scaffold ratio within SPEED, ratios ranged from 0.2:1 to 1:1 (constant
447 scaffold protein 1 mM). Effects of pH (5.0-9.0, 30°C), temperature (30-70°C, pH 7.0), and PET
448 substrate type (PET powder, low and high crystallinity PET films, commercial bottle) were also
449 analyzed.

450 For PET upcycling reaction, PET degrading enzymes (FAST, MHETase, ICCG) were
451 combined with Scaf.4 (1 mM, CipA-CBM-$SH3_D$-ScaB) in an optimized ratio. Similarly, the
452 upcycling enzymes (FucO, AldA, LrNox), which facilitate the synthesis of valuable products from
453 PET, were mixed with Scaf.4 (0.5 mM) in a molar ratio of 1:1. The mixed proteins were incubated
454 at room temperature for 40 minutes to achieve complex assembly. Following assembly, the
455 upcycling complex was incorporated into the PET degradation product, which was reacted for four
456 days under optimal conditions. Alternatively, the PET degradation complex was mixed with the
457 upcycling complex and 100 mg PET Film-L for further conversion. The reactions were conducted
458 in 500 μL systems for 2 to 4 days in SP buffer (with 1 mM additional NADH).

459 For living cell PET degradation, a mixture of 1×10^9 induced *Pichia pastoris* SMD1168 was
460 collected, then placed in 400 μL of sterile glycine-NaOH buffer (pH 7.0) containing 100 mg PET
461 powder to facilitate the degradation reaction. The degradation reaction was conducted at 30°C for
462 48 h.

463 All reactions were terminated at 95°C for 10 min, supernatants were 0.22 μm filtered, and
464 released products were quantified by HPLC (High Performance Liquid Chromatography).

465 **MHETase degradation assay**

466 To assess the intermediates degradation ability of MHETase, 0.5 mM $SH3_L$-optiMHETase was
467 combined with 5 mM MHET and BHET in 500 μL reaction buffer (50 mM sodium phosphate, 0.5
468 mM CaCl2, 10% DMSO, pH 7.0). The reactions were constructed at varying temperatures (30°C,
469 40°C, 50°C, 60°C, 70°C) for 96 h and terminated by heating to 95°C for 10 min. Supernatants were
470 0.22 μm filtered, and released products were quantified by HPLC.

471 **HPLC analysis**

472 TPA, GA, MHET, and BHET standards were obtained from Aladdin (China). Samples were
473 analyzed using an Agilent 1260 LC system with G1315A diode array detector (DAD) and ZORBAX
474 StableBond C18 column (Agilent), refractive index detector (RID) and Xtimate® Sugar-H column
475 (Welch Materials). For TPA, MHET and BHET detection, the mobile phase consisted of 0.1%
476 formic acid (A) and acetonitrile (B); separation used a flow rate of 1 mL/min (80% A / 20% B, 10
477 min); detection was performed at 240 nm with C18 column. For GA detection, the mobile phase
478 consisted of 5 mM H_2SO_4 (Solvent as ddH_2O); separation used a flow rate of 1 mL/min (15 min);
479 detection was performed with Sugar-H column. Analyte concentrations were determined using
480 calibration curves (10-500 mM). Samples were adaptively diluted with ultrapure water prior to
481 analysis.

482 **Scanning electron microscopy (SEM)**

483 Low-crystallinity PET film samples (6 mm diameter) were analyzed by SEM (HuaSuan Technolygy,
484 China) after degradation (40°C, 96 h, pH 7.0). Samples were washed (10% SDS, water, ethanol),
485 dried, gold-coated, and imaged.

486 **Scaffold-enzyme Structural prediction**

487 In this study, the three enzymes structures were obtained from the Protein Data Bank
488 (https://www.rcsb.org/. FAST-PETase: 6IJ6, MHETase: 6QZ4, ICCG: 8JMP, CelK: 3P6B, $SH3_L$:
489 1PRM, ScaA: 5N5P). The structure of the scaffold was predicted by AlphaFold2. After running the
490 standard AlphaFold2 MSA generation pipeline against UniRef, MGnify, PDB, and BFD, the
491 sequence with highest pLDDT greater than 0.9 is chosen as the final model prediction. The
492 prediction of enzyme-scaffold complex was visualized by BioRender (https://www.biorender.com/).

493 **Statistical analysis**

494 One-way analysis of variance (ANOVA) followed by normality test was employed to evaluate the
495 significance of differences among different treatments. Statistical analysis were conducted using
496 GraphPad Prism 9.0 software. ns: not significant, *$p < 0.1$, **$p < 0.01$, ***$p < 0.001$, ****$p <$
497 0.0001.

Declaration of Competing Interest

The authors have two patent applications related to this work.

Data Availability

All data are available in the main text or supplementary information. Additional information related to this study is available from the corresponding author upon reasonable request.

Acknowledgements

This study was supported by funding from the Shenzhen Bay Laboratory Startup Fund, the Shenzhen Outstanding Talents Training Fund, Shenzhen Research Funding for Postdocs and the Key Research and Development Program of Shaanxi Province, China (Grant Numbers: 2022NY-055 and 2019NY-187). We acknowledge the intellectual and experimental contributions of all authors for this study and its manuscript preparation. We are particularly grateful for the insights gained from discussions with lab members in the Zhuobin Liang and Yanbin Lin labs. We would like to acknowledge Ziwei Luo for her technical assistance in the illustration of Figure. 1. We also extend our gratitude to the Haizhen Long and Jianchuan Wang lab at Shenzhen Bay Laboratory for their assistance in experiment setup. Finally, we thank the Research Core Facility of Shenzhen Bay Laboratory for their technical support, especially for the use of ÄKTA and HPLC instruments.

References

1. Lau, W. W. Y. *et al.* Evaluating scenarios toward zero plastic pollution. *Science (1979)* **369**, 1455–1461 (2020).
2. Xu, C. *et al.* Are we underestimating the sources of microplastic pollution in terrestrial environment? *J Hazard Mater* **400**, 123228 (2020).
3. Blackburn, K. & Green, D. The potential effects of microplastics on human health: What is known and what is unknown. *Ambio* **51**, 518–530 (2022).
4. Gao, R., Pan, H., Kai, L., Han, K. & Lian, J. Microbial degradation and valorization of poly(ethylene terephthalate) (PET) monomers. *World J Microbiol Biotechnol* **38**, 89 (2022).
5. Ragaert, K., Delva, L. & Van Geem, K. Mechanical and chemical recycling of solid plastic waste. *Waste Management* **69**, 24–58 (2017).
6. Suzuki, G. *et al.* Global discharge of microplastics from mechanical recycling of plastic waste. *Environmental Pollution* **348**, 123855 (2024).
7. Zeng, W. *et al.* A general strategy for recycling polyester wastes into carboxylic acids and hydrocarbons. *Nat Commun* **15**, 160 (2024).
8. Sullivan, K. P. *et al.* Mixed plastics waste valorization through tandem chemical oxidation and biological funneling. *Science (1979)* **378**, 207–211 (2022).
9. Kushwaha, A., Goswami, L., Singhvi, M. & Kim, B. S. Biodegradation of poly(ethylene terephthalate): Mechanistic insights, advances, and future innovative strategies. *Chemical Engineering Journal* **457**, 141230 (2023).
10. Amalia, L., Chang, C.-Y., Wang, S. S.-S., Yeh, Y.-C. & Tsai, S.-L. Recent advances in the biological depolymerization and upcycling of polyethylene terephthalate. *Curr Opin Biotechnol* **85**, 103053 (2024).
11. Müller, R., Schrader, H., Profe, J., Dresler, K. & Deckwer, W. Enzymatic Degradation of Poly(ethylene terephthalate): Rapid Hydrolyse using a Hydrolase from *T. fusca*. *Macromol Rapid Commun* **26**, 1400–1405 (2005).
12. Sulaiman, S. *et al.* Isolation of a Novel Cutinase Homolog with Polyethylene Terephthalate-Degrading Activity from Leaf-Branch Compost by Using a Metagenomic Approach. *Appl Environ Microbiol* **78**, 1556–1562 (2012).
13. Yoshida, S. *et al.* A bacterium that degrades and assimilates poly(ethylene terephthalate). *Science (1979)* **351**, 1196–1199 (2016).
14. Tournier, V. *et al.* An engineered PET depolymerase to break down and recycle plastic bottles. *Nature* **580**, 216–219 (2020).
15. Lu, H. *et al.* Machine learning-aided engineering of hydrolases for PET depolymerization. *Nature* **604**, 662–667 (2022).
16. Bååth, J. A., Borch, K., Jensen, K., Brask, J. & Westh, P. Comparative Biochemistry of Four Polyester (PET) Hydrolases**. *ChemBioChem* **22**, 1627–1637 (2021).
17. Brizendine, R. K. *et al.* Particle Size Reduction of Poly(ethylene terephthalate) Increases the Rate of Enzymatic Depolymerization But Does Not Increase the Overall Conversion Extent. *ACS Sustain Chem Eng* **10**, 9131–9140 (2022).
18. Chow, J., Perez-Garcia, P., Dierkes, R. & Streit, W. R. Microbial enzymes will offer limited solutions to the global plastic pollution crisis. *Microb Biotechnol* **16**, 195–217 (2023).
19. Carniel, A., Valoni, É., Nicomedes, J., Gomes, A. da C. & Castro, A. M. de. Lipase from Candida antarctica (CALB) and cutinase from Humicola insolens act synergistically for PET

558 hydrolysis to terephthalic acid. *Process Biochemistry* **59**, 84–90 (2017).
559 20. de Castro, A. M., Carniel, A., Nicomedes Junior, J., da Conceição Gomes, A. & Valoni, É.
560 Screening of commercial enzymes for poly(ethylene terephthalate) (PET) hydrolysis and
561 synergy studies on different substrate sources. *J Ind Microbiol Biotechnol* **44**, 835–844
562 (2017).
563 21. Knott, B. C. *et al.* Characterization and engineering of a two-enzyme system for plastics
564 depolymerization. *Proceedings of the National Academy of Sciences* **117**, 25476–25485
565 (2020).
566 22. Barth, M. *et al.* A dual enzyme system composed of a polyester hydrolase and a
567 carboxylesterase enhances the biocatalytic degradation of polyethylene terephthalate films.
568 *Biotechnol J* **11**, 1082–1087 (2016).
569 23. Mrigwani, A., Thakur, B. & Guptasarma, P. Conversion of polyethylene terephthalate into
570 pure terephthalic acid through synergy between a solid-degrading cutinase and a reaction
571 intermediate-hydrolysing carboxylesterase. *Green Chemistry* **24**, 6707–6719 (2022).
572 24. von Haugwitz, G. *et al.* Structural Insights into (Tere)phthalate-Ester Hydrolysis by a
573 Carboxylesterase and Its Role in Promoting PET Depolymerization. *ACS Catal* **12**, 15259–
574 15270 (2022).
575 25. Hwang, D.-H. *et al.* Enhanced biodegradation of waste poly(ethylene terephthalate) using a
576 reinforced plastic degrading enzyme complex. *Science of The Total Environment* **842**,
577 156890 (2022).
578 26. Oliveira, C., Carvalho, V., Domingues, L. & Gama, F. M. Recombinant CBM-fusion
579 technology — Applications overview. *Biotechnol Adv* **33**, 358–369 (2015).
580 27. Makryniotis, K., Nikolaivits, E., Gkountela, C., Vouyiouka, S. & Topakas, E. Discovery of
581 a polyesterase from Deinococcus maricopensis and comparison to the benchmark
582 LCCICCG suggests high potential for semi-crystalline post-consumer PET degradation. *J*
583 *Hazard Mater* **455**, 131574 (2023).
584 28. Duarte, M. *et al.* Structure-function studies can improve binding affinity of cohesin-dockerin
585 interactions for multi-protein assemblies. *Int J Biol Macromol* **224**, 55–67 (2023).
586 29. Arnal, G. *et al.* Assessment of Four Engineered PET Degrading Enzymes Considering
587 Large-Scale Industrial Applications. *ACS Catal* **13**, 13156–13166 (2023).
588 30. Zhang, J. *et al.* Computational design of highly efficient thermostable MHET hydrolases
589 and dual enzyme system for PET recycling. *Commun Biol* **6**, 1135 (2023).
590 31. Wang, X., Lan, P. C. & Ma, S. Metal–Organic Frameworks for Enzyme Immobilization:
591 Beyond Host Matrix Materials. *ACS Cent Sci* **6**, 1497–1506 (2020).
592 32. Kim, H. T. *et al.* Biological Valorization of Poly(ethylene terephthalate) Monomers for
593 Upcycling Waste PET. *ACS Sustain Chem Eng* **7**, 19396–19406 (2019).
594 33. Weiland, F., Kohlstedt, M. & Wittmann, C. Biobased de novo synthesis, upcycling, and
595 recycling — the heartbeat toward a green and sustainable polyethylene terephthalate
596 industry. *Curr Opin Biotechnol* **86**, 103079 (2024).
597 34. Wongsatit, T., Srimora, T., Kiattisewee, C. & Uttamapinant, C. Enzymes, auxiliaries, and
598 cells for the recycling and upcycling of polyethylene terephthalate. *Curr Opin Syst Biol* **38**,
599 100515 (2024).
600 35. Jin, L. *et al.* Gallic acid improves cardiac dysfunction and fibrosis in pressure overload-
601 induced heart failure. *Sci Rep* **8**, 9302 (2018).

36. Ojo, O. A., Rotimi, D. E., Ojo, A. B., Ogunlakin, A. D. & Ajiboye, B. O. Gallic acid abates cadmium chloride toxicity via alteration of neurotransmitters and modulation of inflammatory markers in Wistar rats. *Sci Rep* **13**, 1577 (2023).
37. Mahboob, T. *et al.* PLGA nanoparticles loaded with Gallic acid- a constituent of Leea indica against Acanthamoeba triangularis. *Sci Rep* **10**, 8954 (2020).
38. Montella, C. *et al.* Crystal Structure of an Iron-Dependent Group III Dehydrogenase That Interconverts <scp>l</scp> -Lactaldehyde and <scp>l</scp> -1,2-Propanediol in *Escherichia coli*. *J Bacteriol* **187**, 4957–4966 (2005).
39. Pandit, A. V., Harrison, E. & Mahadevan, R. Engineering Escherichia coli for the utilization of ethylene glycol. *Microb Cell Fact* **20**, 22 (2021).
40. Gao, H. *et al.* NADH oxidase from Lactobacillus reuteri: A versatile enzyme for oxidized cofactor regeneration. *Int J Biol Macromol* **123**, 629–636 (2019).
41. Heyde, S. A. H., Arnling Bååth, J., Westh, P., Nørholm, M. H. H. & Jensen, K. Surface display as a functional screening platform for detecting enzymes active on PET. *Microb Cell Fact* **20**, 93 (2021).
42. Chen, Z. *et al.* Biodegradation of highly crystallized poly(ethylene terephthalate) through cell surface codisplay of bacterial PETase and hydrophobin. *Nat Commun* **13**, 7138 (2022).
43. Chen, Z. *et al.* Enhanced in situ biodegradation of microplastics in sewage sludge using hyperthermophilic composting technology. *J Hazard Mater* **384**, 121271 (2020).
44. Sagong, H.-Y. *et al.* Decomposition of the PET Film by MHETase Using Exo-PETase Function. *ACS Catal* **10**, 4805–4812 (2020).
45. Oda, K. & Wlodawer, A. Development of Enzyme-Based Approaches for Recycling PET on an Industrial Scale. *Biochemistry* (2024) doi:10.1021/acs.biochem.3c00554.
46. Cui, Y. *et al.* Computational Redesign of a PETase for Plastic Biodegradation under Ambient Condition by the GRAPE Strategy. *ACS Catal* **11**, 1340–1350 (2021).
47. Zhong-Johnson, E. Z. L., Voigt, C. A. & Sinskey, A. J. An absorbance method for analysis of enzymatic degradation kinetics of poly(ethylene terephthalate) films. *Sci Rep* **11**, 928 (2021).
48. Bell, E. L. *et al.* Directed evolution of an efficient and thermostable PET depolymerase. *Nat Catal* **5**, 673–681 (2022).
49. Liu, Y. *et al.* Enhancement of the degradation capacity of IsPETase for PET plastic degradation by protein engineering. *Science of The Total Environment* **834**, 154947 (2022).
50. Liu, Z., Zhang, Y. & Wu, J. Enhancement of PET biodegradation by anchor peptide-cutinase fusion protein. *Enzyme Microb Technol* **156**, 110004 (2022).
51. Hayes, H. C. & Luk, L. Y. P. Investigating the effects of cyclic topology on the performance of a plastic degrading enzyme for polyethylene terephthalate degradation. *Sci Rep* **13**, 1267 (2023).
52. Cui, Y. *et al.* Computational redesign of a hydrolase for nearly complete PET depolymerization at industrially relevant high-solids loading. *Nat Commun* **15**, 1417 (2024).

Author information

Authors and Affiliations

College of Life Sciences, Northwest A&F University, Yangling, Shaanxi, China
Yujia Zhang, Chongsen Li, Yanbing Lin

Institute of Molecular Physiology, Shenzhen Bay Laboratory, Shenzhen, China
Yujia Zhang, Chongsen Li, Ehsan Hashimi, Hui Gao, Zhuobin Liang

School of Science, Harbin Institute of Technology (Shenzhen), Shenzhen, China
Enting Xu, Xuemei Yang

Contributions

Yujia Zhang: Methodology, Investigation, Data Curation, Formal Analysis, Visualization, Writing – Original Draft. **Chongsen Li:** Investigation, Data Curation, Validation. **Ehsan Hashimi**: Investigation, Data Curation, Validation. **Enting Xu:** Investigation, Validation. **Xuemei Yang:** Methodology, Supervision, **Yanbing Lin:** Resources, Supervision. **Hui Gao:** Conceptualization, Methodology, Investigation, Data Curation, Formal Analysis, Writing – Original Draft, Funding acquisition. **Zhuobin Liang:** Conceptualization, Methodology, Supervision, Writing – Original Draft, Project administration, Funding acquisition.

Corresponding authors

Correspondence to Zhuobin Liang or Hui Gao.

Extended Data

Source Data

Supplementary information

Supplementary Tables 1-3
Supplementary Figure 1-11
Supplementary File 1
Supplementary Methods

668 **Supplementary Table 1. Key degradation parameters and efficiency of major PET hydrolases**

PET hydrolase	Substrate*	Reaction condition	Enzyme usage (nmol)	Total products (mM)	Degradation efficiency (mol total products /mmol enzyme)	Reference
IsPETase	Film-L	30°C, 18 h, pH 7.0	0.015	0.30	6.00	13
TfH			0.015	0.00079	0.016	
LCC			0.015	0.0063	0.13	
FsC			0.015	0.00075	0.015	
LCC	Post-consumer colored-flake PET waste-H	72°C, 20 h, pH 8.0	690.00	552.09	64.01	14
ICCG (LCC$^{F243I/D238C/S283C/Y127G}$)		72°C, 15 h, pH 8.0	690.00	854.17	99.03	
WCCG (LCC$^{F243W/D238C/S283C/Y127G}$)		72°C, 20 h, pH 8.0	690.00	885.42	102.66	
FAST-PETase (*Is*PETase$^{S121E/D186H/R224Q/N233K/R280A}$)	Film-H	50°C, 96 h, pH 8.0	0.12	33.80	169.00	15
ICCM (LCC$^{F243I/D238C/S283C/N246M}$)			0.12	29.50	147.50	
		40°C, 96 h, pH 8.0	0.12	14.75	73.75	
DuraPETase (*Is*PETase$^{S214H/I168R/W159H/S188Q/R280A/A180I/G165A/Q119Y/L117F/T140D}$)	Film-H	50°C, 72 h, pH 9.0	0.17	2.63	7.56	46
		37°C, 72 h, pH 9.0	0.17	1.76	5.06	
LCC			0.17	1.04	3.00	
TS-PETase (*Is*PETase$^{S121E/D186H/R280A}$)	Film-L	30°C, 6 days, pH 9.0	0.40	0.05	0.13	47
***fv Thermobifida fusca* cutinase$^{H184S/Q92G/F209I/I213K}$**	Bottle-H	60°C, 96 h, pH 8.0	1461.18	N/A (3542.00 nmol)	2.42	42
LCC$^{H184S/Q92G/F209I/I213K}$			1742.22	N/A (1354.00 nmol)	0.78	
BhrPETase$^{H184S/Q92G/F209I/I213K}$			1724.14	N/A (3802.00 nmol)	2.21	
HotPETase	Powder-H	60°C, 5 h, pH 9.2	0.21	6.07	146.52	48
DuraPETase-4M (DuraPETase$^{N233C/S282C/H214S/S245R}$)	Powder-H	60°C, 96 h, pH 9.0	0.01	15.80	45.48	49
DuraPETase			0.01	5.70	16.39	
DSI- *Tf*cutinase$^{D204C/E253C}$ (Tfuc2 fusing with the anchor peptide Dermaseptin SI)	Particle-L	70°C, 96 h, pH 8.0	7.00	300.00	42.86	50
***Is*PETase-Spy (Cyclic monomer)**	Powder-H	30°C, 24 h, pH 7.5	0.10	0.40	4.03	51
***Is*PETase-Dimer (Cyclic dimer)**			0.05	0.46	9.16	
***Is*PETase-Cat (Catenane)**			0.05	0.50	9.95	
***Is*PETase**			0.10	0.40	3.95	
TurboPETase	Film-L	65°C, 12 h, pH 8.0	0.16	130.00	401.04	52
BhrPETase			0.16	6.00	18.54	
LCC^{ICCG}			0.16	34.00	104.41	
FAST-PETase			0.15	2.00	6.89	

669 Note: **a**. * Substrates can vary in different studies. To facilitate their comparison, we define substrates as follows L:
670 low crystallinity (< 20%), H: high crystallinity (> 20%). **b**. Total products include TPA, MHET, and BHET. 3.
671 Extended details associated of this table is provided in **Supplementary File 1**. **c**. N/A: information not available
672 from the corresponding publication.

Supplementary Table 2. Information of genes and primers

Type	Gene	Sequence
Enzyme	FAST-PETase-CelK	catatgcagacaaatccctatgcccgtgggccaaatcccactgcggcgagtttagaagccagtgccggtccgtttaccgtccgttcttttactgtaagccgcccgtccggata cggggcggggacggtttattatcccacgaatgccggaggcaccgtgggtgctattgcaattgttccaggctatacagcgcgccaatcatctatcaaatggtggggaccgcg tctggcttcgcacggattcgtagttattacgattgacacaaacagcacgttagaccagcccgaaagtcgcagcagtcaacaaatggcggcgttacgtcaggtcgcaagctta aacgggacatcaagcagtcccatctatggaaaagtcgatacagcgcgcatgggtgtcatgggctggtccatgggaggcgggggtctttgatttctgctgctaataatccta gtttaaaagccgccgccccgcaggcaccgtggcattcgtccaccaacttttcatcggtaacggtccccactcttatttttgcgtgtgagaacgactcgatcgcaccggttaatt cttctgctctgccgatttacgactcaatgtcgcaaaatgcaaagcaattccttgaaattaaaggtggctcccattcttgtgccaactcaggtaacagtaatcaagcccttattgga aagaaaggtgtcgcatggatgaaacgttttatggataatgacacccgctattctaccttcgcctgcgaaaacccgaacagcaccgctgtatcagatttccgcactgccaactg tagcttaataacaccgccaggaggagtagacccagaagaaccggaggttatttatggtgactgcaatggcgacggaaaagttaattcaactgacgctgtggcattgaagag atatatcttgagatcaggtataagcatcaacactgataatgctgatgtaaatgctgatggcagagttaactctacagacttggcaatattgaagagatatattcttaaagagatag atgtattgccacataaactcgag
Enzyme	MHETase-CelF	catatgcagaccacagtaacgacgatgttgcttgcaagcgtagccttagccgcctgtgcgggtggtggcagcaccccattaccgttaccgcaacaacagccgccccagca agaaccacccccaccgcctgtcccgttagcgtcacgcgcagcatgtgaggcactgaaagacggcaatggcgacatggtatggccgaatgccgctaccgtggtcgaagtc gctgcctggcgcgacgcggcaccagctacagcaagtgctgctgcactgcctgaacactgcgaagtgtcgggcgcgatcgcgaaacgcacgggcattgatggctacccg tacgaaattaaatttcgtcttcgtatgccagcggaatggaatggacgtttcttcatggagggcggctcggggacaaatggttcattgtcagcggctacaggttcgattgggggt ggtcaaattgcatctgccttgagccgcaacttcgccaccatcgctaccgacggagggcatgataacgcggttaatgacaacccggatgcattgggaacagttgcctttggttt agatccccaggctcgtctggacatgggctacaatagttacgaccaggtcacgcaagctggcaaggctgcggttgctcgtttctatggacgtgcggcagacaaatcgtatttc attggatgcagtgagggaggacgcgagggcatgatgctgagccagcgctttccatcacactacgatggcattgtcgccggtgcccctgggtatcagctgccaaaagccg ggatttccggtgcctggacgacgcaatccttggcaccagccgcagtcgggttagatgcgcaaggggtgcctctgattaataagtccttctcggatgctgatttgcaccttctgt cacaagctatcttaggaacatgtgacgctctggatggattggcagatggaattgttgacaactaccgcgcctgtcaggcagcgttcgatcccgctacagctgcgaatccggc taacggtcaggccttgcaatgtgtcggggcaaagacagcagactgcctgtctcctgtgcaggtgaccgctatcaaacgcgcgatggcagggccagtgaattctgcaggca ccccccctgtataatcgttgggcgtgggacgctggtatgagtggcttgtcagggacaacgtataatcagggatggcgcagctggtggttggggtctttcaacagctctgcgaa taacgcgcaaaaggtcagcggcttcgcggctcgttcctggctggtggatatcgcaactccaccagagcccatgcctatgacccaggttgctgcacgcatgatgaaattcga cttcgatattgatccgctgaaaatttgggcgacatctgggcaatttacacaaagctctatggactggcacggcgctacttcgaccgatttagcggctttttcgtgaccgtggagg caagatgatcttgtatcacggtatgagtgatgcggccttcagtgcattagatacggcggattattacgagcgtctgggagcggctatgcctggggctgccggtttcgctcgcc ttttttagtaccagggatgaaccattgctcaggcgggcctggaacggaccgttttgacatgttgactcctttagtggcctgggttgagcgtggcgaggcgcctgatcaaatttc cgcatggtccgggaccccagggtatttcggtgttgcagcacgcacccgcccgttgtgtccatatccacaaatcgcgcgttataaagggtccggagacattaatacggaagc gaattttgcttgcgcagcccccccctcccagatcaaggtccagaaaaattattgggtgatgtaaacggtgacgaactgtagacgctattgaccttgctatacttaaaaaatat cttttaaacagcagtactacaataaatactgcaaatgcagatatgaatagtgataatgctattgacgctattgactatgctcttttaaagaaagcacttctttctatccaactcgag
Enzyme	optiMHETase-CelF	ggtggtggtagtacaccgctgccgctgcctcagcagcagcctccgcagcaagaaccgcctccgcctccggttccgctggcaagccgtgcagcatgtgaagcactgaaa gatggtaatggtgatatggtttggccgaatgcagcaaccgttgttgaagttgcagcatggcgtgatgcagcaccggcaaccgcaagcgcagcagcactgccggaacattg tgaagttagcggtgcaattgccaaacgtaccggtattgatggttatccgtatgaaatcaaatttcgtctgcgtatgcctgcagaatggaatggtcgtttctttatggaaggtggta gcggcaccaatggtagcctgagcgcagccaccggtagcattggtggtggtcagattgcaagcgcactgagccgtaattttgcaaccattgcaaccgatggtggtcatgata atgccgttaatgataatccggatgcactgggcaccgttgcatttggtctggatccgcaggcacgtctggatatgggttataatagctatgatcaggttacccaggcaggtaaa gcagcagttgcacgtttttatggtcgtgcagcagataaaagctattttatcggttgtagcgaaggtggtcgtgaaggtatgatgctgagccagcgttttccgagccattatgatg gtattgttgcgggtgcaccgggttatcagctgccgaaagcaggtattagtggtgcatggaccacacagagcctggcaccggcagccgttggcctggatgcacagggtgtt ccgctgattaacaaaagctttagtgatgccgatctgcatctgctgagtcaggcaattctgggcacctgtgatgccctggatggtctggcagatggcattgttgataactatcgtg catgtcaggcagcatttgatccggcaacagcagcaaatccggcaaatggtcaggccctgcagtgtgttggtgcaaaaaccgcagattgtctgagtccggttcaggtgaccg caattaaacgcgcaatggcaggtccggttaatagcgcaggcacaccgctgtataatcgttgggcatgggatgcaggtatgagcggtctgagcggtacaacctataatcaag gttggcgtagttggtggctgggtagctttaatagcagcgcaaataatgcccagcgtgttagcggttttagcgcacgtagctggctggttgattttgcgacccctccggaaccg atgccgatgacacaggttgcagcacgcatgatgaaattcgattttgatattgacccgctgaaaatttgggcaaccagcggtcagtttacccagagtagcatggattggcatgg tgcaaccagcaccgatctggcagcctttcgtgatcgtggtggtaaaatgattctgtatcatggtatgtcagatgcagcctttagtgcactggatacagcagattattatgaacgt ctgggtgcagcaatgcctggtgcagcaggttttgcacgtctgtttctggttccgggtatgaatcattgtagcggtggtccgggtacagatcgttttgatatgctgacccctctgg ttgcatgggttgaacgtggtgaagcaccggatcagattagcgcatggtcaggtactccgggttattttggtgttgccgcacgtacccgtccgctgtgtccgtatccgcagatc gcacgttataaaggtagcggtgatattaacaccgaagccaattttgcatgtgcagcacctccgttcccagatcaaggtccagaaaaattattgggtgatgtaaacggtgacga aactgtagacgctattgaccttgctatacttaaaaaatatctttaaacagcagtactacaataaatactgcaaatgcagatatgaatagtgataatgctattgacgctattgactat gctcttttaaagaaagcacttctttctatccaa
Enzyme	$SH3_L$-optiMHETase	cctcctcctgctctgccaccaaaaaggagaagacatcatcatcatcatcacagcagcggcctggtgccgcgcggcagcggtggtggtagtacaccgctgccgctgcctca gcagcagcctccgcagcaagaaccgcctccgcctccggttccgctggcaagccgtgcagcatgtgaagcactgaaagatggtaatggtgatatggtttggccgaatgca gcaaccgttgttgaagttgcagcatggcgtgatgcagcaccggcaaccgcaagcgcagcagcactgccggaacattgtgaagttagcggtgcaattgccaaacgtaccg gtattgatggttatccgtatgaaatcaaatttcgtctgcgtatgcctgcagaatggaatggtcgtttctttatggaaggtggtagcggcaccaatggtagcctgagcgcagcca ccggtagcattggtggtggtcagattgcaagcgcactgagccgtaattttgcaaccattgcaaccgatggtggtcatgataatgccgttaatgataatccggatgcactgggc accgttgcatttggtctggatccgcaggcacgtctggatatgggttataatagctatgatcaggttacccaggcaggtaaagcagcagttgcacgtttttatggtcgtgcaga gataaaagctattttatcggttgtagcgaaggtggtcgtgaaggtatgatgctgagccagcgttttccgagccattatgatggtattgttgcgggtgcaccgggttatcagctgc cgaaagcaggtattagtggtgcatggaccacacagagcctggcaccggcagccgttggcctggatgcacagggtgttccgctgattaacaaaagctttagtgatgccgatc tgcatctgctgagtcaggcaattctgggcacctgtgatgccctggatggtctggcagatggcattgttgataactatcgtgcatgtcaggcagcatttgatccggcaacagca gcaaatccggcaaatggtcaggccctgcagtgtgttggtgcaaaaaccgcagattgtctgagtccggttcaggtgaccgcaattaaacgcgcaatggcaggtccggtgtaat agcgcaggcacaccgctgtataatcgttgggcatgggatgcaggtatgagcggtctgagcggtacaacctataatcaaggttggcgtagttggtggctgggtagctttaata gcagcgcaaataatgcccagcgtgttagcggttttagcgcacgtagctggctggttgattttgcgacccctccggaaccgatgccgatgacacaggttgcagcacgcatga tgaaattcgattttgatattgacccgctgaaaatttgggcaaccagcggtcagtttacccagagtagcatggattggcatggtgcaaccagcaccgatctggcagcctttcgtg atcgtggtggtaaaatgattctgtatcatggtatgtcagatgcagcctttagtgcactggatacagcagattattatgaacgtctgggtgcagcaatgcctggtgcagcaggttttgcacgtctgtttctggttccgggtatgaatcattgtagcggtggtccgggtacagatcgttttgatatgctgacccctctggttgcatgggttgaacgtggtgaagcaccggatcagattagcgcatggtcaggtactccgggttattttggtgttgccgcacgtacccgtccgctgtgtccgtatccgcagatcgcacgttataaaggtagcggtgatattaacaccgaagccaattttgcatgtgcagcacctccg
Enzyme	OptiMHETase-$SH3_L$	ggtggtggtagtacaccgctgccgctgcctcagcagcagcctccgcagcaagaaccgcctccgcctccggttccgctggcaagccgtgcagcatgtgaagcactgaaa gatggtaatggtgatatggtttggccgaatgcagcaaccgttgttgaagttgcagcatggcgtgatgcagcaccggcaaccgcaagcgcagcagcactgccggaacattg tgaagttagcggtgcaattgccaaacgtaccggtattgatggttatccgtatgaaatcaaatttcgtctgcgtatgcctgcagaatggaatggtcgtttctttatggaaggtggta gcggcaccaatggtagcctgagcgcagccaccggtagcattggtggtggtcagattgcaagcgcactgagccgtaattttgcaaccattgcaaccgatggtggtcatgata atgccgttaatgataatccggatgcactgggcaccgttgcatttggtctggatccgcaggcacgtctggatatgggttataatagctatgatcaggttacccaggcaggtaaa gcagcagttgcacgtttttatggtcgtgcagcagataaaagctattttatcggttgtagcgaaggtggtcgtgaaggtatgatgctgagccagcgttttccgagccattatgatg gtattgttgcgggtgcaccgggttatcagctgccgaaagcaggtattagtggtgcatggaccacacagagcctggcaccggcagccgttggcctggatgcacagggtgtt ccgctgattaacaaaagctttagtgatgccgatctgcatctgctgagtcaggcaattctgggcacctgtgatgccctggatggtctggcagatggcattgttgataactatcgtg catgtcaggcagcatttgatccggcaacagcagcaaatccggcaaatggtcaggccctgcagtgtgttggtgcaaaaaccgcagattgtctgagtccggttcaggtgaccg caattaaacgcgcaatggcaggtccggttaatagcgcaggcacaccgctgtataatcgttgggcatgggatgcaggtatgagcggtctgagcggtacaacctataatcaag gttggcgtagttggtggctgggtagctttaatagcagcgcaaataatgcccagcgtgttagcggttttagcgcacgtagctggctggttgattttgcgacccctccggaaccg atgccgatgacacaggttgcagcacgcatgatgaaattcgattttgatattgacccgctgaaaatttgggcaaccagcggtcagtttacccagagtagcatggattggcatgg tgcaaccagcaccgatctggcagcctttcgtgatcgtggtggtaaaatgattctgtatcatggtatgtcagatgcagcctttagtgcactggatacagcagattattatgaacgt ctgggtgcagcaatgcctggtgcagcaggttttgcacgtctgtttctggttccgggtatgaatcattgtagcggtggtccgggtacagatcgttttgatatgctgacccctctgg ttgcatgggttgaacgtggtgaagcaccggatcagattagcgcatggtcaggtactccgggttattttggtgttgccgcacgtacccgtccgctgtgtccgtatccgcagatc gcacgttataaaggtagcggtgatattaacaccgaagccaattttgcatgtgcagcacctccgcaccaccaccaccaccaccctcctcctgctctgccaccaaaaaggagaaga

Type	Gene	Sequence
Enzyme	ICCG-ScaA	agcaacccgtaccagcgtggcccgaatccgacccgcagcgcactgaccgcagatggcccgtttagcgtggcaacctacaccgtctcacgcctgtcagtctcgggttttgg cggtggcgtgatttattacccgaccggcacgtctctgacgttcggtggcatcgcgatgagtccgggttataccgcagatgctagctctctggcatggctgggtcgtcgcctg gcttcccatggctttgtggttctggtgattaacacgaattcacgtttcgatggcccggacagccgcgcctctcagctgagtgccgccctgaactacctgcgtaccagttcccc gagcgccgttcgcgcacgtctggatgcaaatcgtctggcggttgccggtcattctatgggtggcggtggcaccctgcgtattgcagaacaaacccgagcctgaaagcgg ctgtcccgctgaccccgtggcacaccgataaaacgtttaataccagtgtcccggtgctgattgttggcgcagaagctgacaccgtggcgccggtttcgcagcatgccatcc cgttttatcaaaacctgccgagcaccacgccgaaagtttacgtcgaactgtgcaacgcatcgcacattgctccgaacagcaacaatgcggccatttccgtttatacgatctcat ggatgaaactgtgggtcgataatgacacccgttaccgccagttcctgtgtaatgtgaacgacccggctctgtgcgacttccgcaccaataatcgccactgccaagtaacaac tcctcagcccggcacaaagctcgttcctacatggggcgatacaaactgcgacggcgttgtaaatgttgctgacgtagtagttcttaacagattcctcaacgatcctacatattct aacattactgatcagggtaaggttaacgcagacgttgttgatcctcaggataagtccggcgcagcagttgatcctgcaggcgtaaagctcacagtagctgactctgaggcaa tcctcaaggctatcgttgaa
Enzyme	FucO-CelF	atgatggctaacagaatgctggtgaacgaaacggcatggtttggtcgaggtgctgttggagctttaaccgatgaagtgaaacgccgtggttatcagaaggcgctgatcgtca ccgataaaacgctggtgcaatgcggcgtggtggcgaaagtgaccgacaagatggatgccgcaggactggcatgggcgatttacgacggcgtagtacctaacccaacaat tactgtcgtcaaagaagggctcgatgtattccagaatagcggcgcggattacctgatcgctattggtggtggttctccacaggatacgtgtaaagcgattggcattatcagca acaacccggagtttgccgatgtgcgtagcctggaagggctttccccgaccaataaacccagtgtaccgattctggcaatccccaccacagcaggcactgcggcagaagtg accattaactacgtgatcactgacgaagagaaacggcgcaagtttgtttgcgttgatccgcatgatatcccgcaggtggcgtttattgacgctgacatgatggatggtatgcct ccagcgctgaaagctgcgacgggtgtcgatgcgctcactcatgctattgaggggtatattacccgtggcgcgtgggcgctaaccgatgcactgcacattaaagcgattgaa atcattgctgggcgctgcgaggatcggttgctggtgataaggatgccggagaagaaatggcgctcgggcagtatgttgcgggtatgggcttctcgaatgttgggttaggg ttggtgcatggtatggcgcatccactgggcgcgttttataacactccacacggtgttgcgaacgccatcctgttaccgcatgtcatgcgttataacgctgactttaccggtgag aagtaccgcgatatcgcgcgcgttatgggcgtgaaagtggaaggtatgagcctggaagaggcgcgtaatgccgccgttgaagcggtgtttgctctcaaccgtgatgtcggt attccgccacatttacgtgatgttggtgtacgcaaggaagacattccggcactggcgcaggcggcactggatgatgtttgtaccggtggcaacccgcgtgaagcaacgctt gaggatattgtagagctttaccataccgcctggtctggaggtggaggctcaggaggtggaggctctggaggtggaggctcaggaggtggaggctcacctaggttcccag atcaaggtccagaaaaattattgggtgatgtaaacggtgacgaaactgtagacgctattgaccttgctatacttaaaaaatatcttttaaacagcagtactacaataaatactgca aatgcagatatgaatagtgataatgctattgacgctattgactatgctcttttaaagaaagcacttctttctatccaactcgag
Enzyme	$SH3_L$-AldA	cctcctcctgctctgccaccaaaaaggagaagatctggaggtggaggctcaggaggtggaggctccggaggtggaggctcacatatgtcagtacccgttcaacatcctat gtatatcgatggacagtttgttacctggcgtggagacgcatggattgatgtggtaaaccctgctacagaggctgtcatttcccgcatacccgatggtcaggccgaggatgcc cgtaaggcaatcgatgcagcagaacgtgcacaaccagaatgggaagcgttgcctgctattgaacgcgccagttggttgcgcaaaatctccgccgggatccgcgaacgcg ccagtgaaatcagtgcgctgattgttgaagaagggggcaagatccagcagctggctgaagtcgaagtggcttttactgccgactatatcgattacatggcggagtgggcac ggcgttacgagggcgagattattcaaagcgatcgtccaggagaaaatattcttttgtttaaacgtgcgcttggtgtgactaccggcattctgccgtggaacttcccgttcttcctc attgcccgcaaaatggctcccgctcttttgaccggtaataccatcgtcattaaacctagtgaatttacgccaaacaatgcgattgcattcgccaaaatctgtcgatgaaataggc cttccgcgcggcgtgtttaacctgtactggggcgtggtgaaaccgttgggcaagaactggcgggtaacccaaaggtcgcaatggtcagtatgacaggcagcgtctctgca ggtgagaagatcatggcgactgcggcgaaaaacatcaccaaagtgtgtctggaattgggggggtaaagcaccagctatcgtaatggacgatgccgatcttgaactggcagt caaagccatcgttgattcacgcgtcattaatagtgggcaagtgtgtaactgtgcagaacgtgtttatgtacagaaaggcatttatgatcagttcgtcaatcggctgggtgaagc gatgcaggcggttcaatttggtaaccccgctgaacgcaacgacattgcgatggggccgttgattaacgccgcggcgctggaaagggtcgagcaaaaagtggcgcgcgc agtagaagaagggggcgagagtggcgttcggtggcaaagcggtagaggggaaaggatattattatccgccgacattgctgcttggatgttcgccaggaaatgtcgattatgc atgaggaaacctttggcccggtgctgccagttgtcgcatttgacacgctggaagatgctatctcaatggctaatgacagtgattacggcctgacctcatcaatctatacccaaa atctgaacgtcgcgatgaaagccattaaagggctgaagtttggtgaaacttacatcaaccgtgaaaacttcgaagctatgcaaggcttccacgccggatggcgtaaatccgg tattggcggcgcagatggtaaacatggcttgcatgaatatctgcagacccaggtggtttatttacagtcgctcgag
Enzyme	LrNox-ScaA	atgaaggttattattgttggttgtacacatgcgggaacaattactgccactcaaattttacagaatcatccagaaacagaagtcacaatttatgaacggaatgataacgtttcattc ctctcatgtgggattgcagtttacttgagcggtgatgttggtaatccagatgcgatgttttattcaagccctgaacaacttgctgccatgggtgcaacagttcatatgcaacataat gtaactgatattgaccctaagactaagacagtcacagtgacagaccttgtgacaggcgaaacaaagaccgaccattatgataagttagttgatactactggttcttggccagta attccaccaattgaaggtgtagatggccctcatgtttatttgtgcaagaattaccatcatgctaaagaattatttaacgttgctaaagatgcgcaacgaattgttgtgattggtgga ggttatattgggttgaattagtagaagcttacactcgtcaaaataaggacgttacattgattgatgggtctccacggatgcttcataaatactttgaccgcgagtatacggatcg aattcaacaggaatttgtagatcacggcgcccactttgcttttgaccaacgcgtaactggatttgaaaaccacgaaaatggtgtaaccgttaagacggataagggcaactacg aggcagatattgctatcctctgtgttggcttccgtcctaatactgatctcttaaaaggtaaagttaagatgcatgataatggggcaatcattacgaacgaatacatgcaatcatct gatccagatatttacgctgccggagattcaacggctgttcactataacccaactggcaaggatgcatacattccattagctactaacgctattcggcaaggaacaattgttgga acaaatctctttggtaatacaatgcgcgatatgggaacccaatctagttctggcttaaacttatatggaacaacgatggtatcatctggcttaactttggagaatgccaaagaag cgggctttgatgcagctgcggtgacagttgaagacaactaccgtccagaatttatgccgacaacaactcctgtattaatgacattggtgtgggataagaagactcggcaaatt cttggtggacagtttatgagtaagcatgatgtttctcaatctgctaacattatttccttatgtatccaggataagcacacgattgattatttagcatttgttgatatgcttttccaaccac actttgatcgtccatttaactatgtaaatattcttggccaagcggcggtaaagaaacaagctgaattagaaaaatctggaggtggaggctcaggaggtggaggctccggagg tggaggctcacctagggtaacaactcctcagcccggcacaaagctcgttcctacatggggcgatacaaactgcgacggcgttgtaaatgttgctgacgtagtagttcttaac agattcctcaacgatcctacatattctaacattactgatcagggtaaggttaacgcagacgttgttgatcctcaggataagtccggcgcagcagttgatcctgcaggcgtaaag ctcacagtagctgactctgaggcaatcctcaaggctatcgttgaactcatcacacttcctcagctcgag
Scaffold	CipA-linker- CipC	ggtgtggtagtagaaattggcaaagttacgggatctgttggaactacagttgaaatacctgtatatttcagaggagttccatccaaaggaatagcaaactgcgactttgtgttca gatatgatccgaatgtattggaaattatagggatagatcccggagacataatagttgacccgaatcctaccaagagctttgatactgcaatatatcctgacagaaagataatag tattcctgtttgcggaagacagcggaacaggagcgtatgcaataactaaagacggagtatttgcaaaaataagagcaactgtaaaatcaagtgctccgggctatattactttc gacgaagtaggtggatttgcagataatgacctggtagaacagaaggtatcatttatagacggtggtgttaacgttggcaatgcaacaccgaccaagggagcaacaccaaca aatacagctacgccgacaaaatcagctacggctacgcccaccaggccatcggtaccgacaaacacaccgacaaacacaccggcaaatacaccgggcagtgtagtacca tcaacacagcctgtaacaacaccacctgcaacaacaaaaccacctgcaacaacaaaaccacctgcaacaacaataccgccgtcagatgatccggcgattctcttaaagtt acagtaggaacagctaatggtaagcctggcgatacagtaacagttcctgttacatttgctgatgtagcaaagatgaaaaacgtaggaacatgtaatttctatcttggatatgatg caagcctgttagaggtagtatcagtagatgcaggtccaatagttaagaatgcagcagttaacttctcaagcagtgcaagcaacggaacaatcagcttcctgttcttggataac acaattacagacgaattgataactgcagacggtgtgtttgcaaatattaagttcaaattaaagagtgtaacggctaaaactacaacaccagtaacatttaaagatggtggagctt tttggtgacggaactatgtcaaagatagcttcagttactaagacaaacggtagtgtaactatagatcctggtactcaa
Scaffold	CipA-linker- CBM-linker- CipC	ggtgtggtagtagaaattggcaaagttacgggatctgttggaactacagttgaaatacctgtatatttcagaggagttccatccaaaggaatagcaaactgcgactttgtgttca gatatgatccgaatgtattggaaattatagggatagatcccggagacataatagttgacccgaatcctaccaagagctttgatactgcaatatatcctgacagaaagataatag tattcctgtttgcggaagacagcggaacaggagcgtatgcaataactaaagacggagtatttgcaaaaataagagcaactgtaaaatcaagtgctccgggctatattactttc gacgaagtaggtggatttgcagataatgacctggtagaacagaaggtatcatttatagacggtggtgttaacgttggcaatgcaacaccgaccaagggagcaacaccaaca aatacagctacgccgacaaaatcagctacggctacgcccaccaggccatcggtaccgacaaacacaccgacaaacacaccggcaaatacaccggtatcaggcaatttga aggttgaattctacaacagcaatccttcagatactactaactcaatcaatcctcagttcaaggttactaataccggaagcagtgcaattgatttgtccaaactcacattgagatatt attatacagtagacggacagaaagatcagaccttctggtgtgaccatgctgcaataatcggcagtaacggcagctacaacggaattacttcaaatgtaaaaggaacatttgta aaaatgagttcctcaacaaataacgcagacacctaccttgaaataagctttacaggcggaactcttgaaccgggtgcacatgttcagatacaaggtagatttgcaaagaatga ctggagtaactatacacagtcaaatgactactcattcaagtctgcttcacagtttgttgaatgggatcaggtaacagcatacttgaacggtgttcttgtatggggtaaagaaccc ggtggcagtgtagtaccatcaacacagcctgtaacaacaccacctgcaacaacaaaaccacctgcaacaacaaaaccacctgcaacaacaataccgccgtcagatgatc cggcgattctcttaaagttacagtaggaacagctaatggtaagcctggcgatacagtaacagttcctgttacatttgctgatgtagcaaagatgaaaaacgtaggaacatgta atttctatcttggatatgatgcaagcctgttagaggtagtatcagtagatgcaggtccaatagttaagaatgcagcagttaacttctcaagcagtgcaagcaacggaacaatca gcttcctgttcttggataacacaattacagacgaattgataactgcagacggtgtgtttgcaaatattaagttcaaattaaagagtgtaacggctaaaactacaacaccagtaac atttaaagatggtggagcttttggtgacggaactatgtcaaagatagcttcagttactaagacaaacggtagtgtaactatagatcctggtactcaactcgag
Scaffold	CipA-linker- CBM-linker- CipC-SED1	ggtgtggtagtagaaattggcaaagttacgggatctgttggaactacagttgaaatacctgtatatttcagaggagttccatccaaaggaatagcaaactgcgactttgtgttca gatatgatccgaatgtattggaaattatagggatagatcccggagacataatagttgacccgaatcctaccaagagctttgatactgcaatatatcctgacagaaagataatag tattcctgtttgcggaagacagcggaacaggagcgtatgcaataactaaagacggagtatttgcaaaaataagagcaactgtaaaatcaagtgctccgggctatattactttc gacgaagtaggtggatttgcagataatgacctggtagaacagaaggtatcatttatagacggtggtgttaacgttggcaatgcaacaccgaccaagggagcaacaccaaca aatacagctacgccgacaaaatcagctacggctacgcccaccaggccatcggtaccgacaaacacaccgacaaacacaccggcaaatacaccggtatcaggcaatttga aggttgaattctacaacagcaatccttcagatactactaactcaatcaatcctcagttcaaggttactaataccggaagcagtgcaattgatttgtccaaactcacattgagatatt attatacagtagacggacagaaagatcagaccttctggtgtgaccatgctgcaataatcggcagtaacggcagctacaacggaattacttcaaatgtaaaaggaacatttgta aaaatgagttcctcaacaaataacgcagacacctaccttgaaataagctttacaggcggaactcttgaaccgggtgcacatgttcagatacaaggtagatttgcaaagaatga

		ctggagtaactatacacagtcaaatgactactcattcaagtctgcttcacagtttgttgaatgggatcaggtaacagcatacttgaacggtgttcttgtatggggtaaagaaccc ggtggcagtgtagtaccatcaacacagcctgtaacaacaccacctgcaacaacaaaaccacctgcaacaacaaaaccacctgcaacaacaatacccgccgtcagatgatc cggcgattctcttaaagttacagtaggaacagctaatggtaagcctggcgatacagtaacagttcctgttacatttgctgatgtagcaaagatgaaaaacgtaggaacatgta atttctatcttggatatgatgcaagcctgttagaggtagtatcagtagatgcaggtccaatagttaagaatgcagcagttaacttctcaagcagtgcaagcaacggaacaatca gcttcctgttcttggataacacaattacagacgaattgataactgcagacggtgtgtttgcaaatattaagttcaaattaaagagtgtaacggctaaaactacaacaccagtaac atttaaagatggtggagcttttggtgacggaactatgtcaaagatagcttcagttactaagacaaacggtagtgtaactatagatcctggtactcaactcgaggggtggtggagg tagtggaggaggtggtagtcaattttccaacagtacatctgcttcttccaccgatgtcacttcctcctcttccatctccacttcctctggctcagtaactatcacatcttctgaagct ccagaatccgacaacggtaccagcacagctgcaccaactgaaacctcaacagaggctccaaccactgctatcccaactaacggtacctctactgaagctccaaccactgc tatcccaactaacggtacctctactgaagctccaactgatactactactgaagctccaaccaccgctcttccaactaacggtacttctactgaagctccaactgatactactct gaagctccaaccaccggtcttccaaccaacggtaccacttcagctttcccaccaactacatctttgccaccaagcaacactaccaccactcctccttacaacccatctactgac tacaccactgactacactgtagtcactgaatatactacttactgtccagaaccaaccactttcaccacaaacggtaagacttacaccgtcactgaaccaaccacattgactatc actgactgtccatgcaccattgaaaagccaacaaccacatcaaccaccgaatacactgtagtcactgagtacactacttactgtccagaaccaaccactttcaccacaaacg gtaagacttacaccgtcactgaaccaaccactttgactatcactgactgtccatgtactattgaaaagagcgaagcccctgagtcttctgtcccagttaccgaatctaagggca ctaccaccaaagaaacaggtgttactaccaaacaaaccacagccaacccaagtctaaccgtctccacagtcgtcccagtttcatcctctgcttcttctcattccgttgtcatcaa cagtaacggtgctaacgtcgtcgttccaggtgctttaggtttggctggtgttgctatgttattcttataa
Scaffold	CipA-linker- CBM-linker- $SH3_D$	ggtgtggtagtagaaattggcaaagttacgggatctgttggaactacagttgaaatacctgtatatttcagaggagttccatccaaaggaatagcaaactgcgactttgtgttca gatatgatccgaatgtattggaaattatagggatagatcccggagacataatagttgacccgaatcctaccaagagctttgatactgcaatatatcctgacagaaagataatag tattcctgtttgcggaagacagcggaacaggagcgtatgcaataactaaagacggagtatttgcaaaaataagagcaactgtaaaatcaagtgctccgggctatattactttc gacgaagtaggtggatttgcagataatgacctggtagaacagaaggtatcatttatagacggtggtgttaacgttggcaatgcaacaccgaccaagggagcaacaccaaca aatacagctacgccgacaaaatcagctacggctacgcccaccaggccatcggtaccgacaaacacaccgacaaacacaccggcaaatacaccggtatcaggcaatttga aggttgaattctacaacagcaatccttcagatactactaactcaatcaatcctcagttcaaggttactaataccggaagcagtgcaattgatttgtccaaactcacattgagatatt attatacagtagacggacagaaagatcagaccttctggtgtgaccatgctgcaataatcggcagtaacggcagctacaacggaattacttcaaatgtaaaaggaacatttgta aaaatgagttcctcaacaaataacgcagacacctaccttgaaataagctttacaggcggaactcttgaaccgggtgcacatgttcagatacaaggtagatttgcaaagaatga ctggagtaactatacacagtcaaatgactactcattcaagtctgcttcacagtttgttgaatgggatcaggtaacagcatacttgaacggtgttcttgtatggggtaaagaaccc ggtggcagtgtagtaccatcaacacagcctgtaacaacaccacctgcaacaacaaaaccacctgcaacaacaaaaccacctgcaacaacaatacccgccgtcagatgatc cggaagaggcagaatatgttcgtgccctgtttgattttaatggcaacgatgaagaagatctgccgtttaaaaagggtgatattctgcgtattcgtgacaaaccggaagaacagt ggtggaatgcagaagatagcgaaggtaaacgtggtatgattccggttccgtatgttgaaaaatatcgtccg
Scaffold	CipA-linker- CBM-linker- $SH3_D$ -ScaB	ggtgtggtagtagaaattggcaaagttacgggatctgttggaactacagttgaaatacctgtatatttcagaggagttccatccaaaggaatagcaaactgcgactttgtgttca gatatgatccgaatgtattggaaattatagggatagatcccggagacataatagttgacccgaatcctaccaagagctttgatactgcaatatatcctgacagaaagataatag tattcctgtttgcggaagacagcggaacaggagcgtatgcaataactaaagacggagtatttgcaaaaataagagcaactgtaaaatcaagtgctccgggctatattactttc gacgaagtaggtggatttgcagataatgacctggtagaacagaaggtatcatttatagacggtggtgttaacgttggcaatgcaacaccgaccaagggagcaacaccaaca aatacagctacgccgacaaaatcagctacggctacgcccaccaggccatcggtaccgacaaacacaccgacaaacacaccggcaaatacaccggtatcaggcaatttga aggttgaattctacaacagcaatccttcagatactactaactcaatcaatcctcagttcaaggttactaataccggaagcagtgcaattgatttgtccaaactcacattgagatatt attatacagtagacggacagaaagatcagaccttctggtgtgaccatgctgcaataatcggcagtaacggcagctacaacggaattacttcaaatgtaaaaggaacatttgta aaaatgagttcctcaacaaataacgcagacacctaccttgaaataagctttacaggcggaactcttgaaccgggtgcacatgttcagatacaaggtagatttgcaaagaatga ctggagtaactatacacagtcaaatgactactcattcaagtctgcttcacagtttgttgaatgggatcaggtaacagcatacttgaacggtgttcttgtatggggtaaagaaccc ggtggcagtgtagtaccatcaacacagcctgtaacaacaccacctgcaacaacaaaaccacctgcaacaacaaaaccacctgcaacaacaatacccgccgtcagatgatc cggaagaggcagaatatgttcgtgccctgtttgattttaatggcaacgatgaagaagatctgccgtttaaaaagggtgatattctgcgtattcgtgacaaaccggaagaacagt ggtggaatgcagaagatagcgaaggtaaacgtggtatgattccggttccgtatgttgaaaaatatcgtccgggatccgccggtggtttatccgctgtgcagcctaatgttagtt taggcgaagtactggatgtttctgctaacagaaccgctgctgacggaacagttgaatggcttatcccaacagtaactgcagctccaggccagacggtcactatgcccgtagt agtcaagagttcaagtcttgcagttgctggtgcgcagttcaagatccaggcggcgacaggcgtacgttattcgtccaagacggacggtgacgcttacggttcaggcattgtg tacaataatagtaagtatgcttttggacagggtgcaggtagaggaatagttgcagctgatgattcggttgtgcttactcttgcatatacagttcccgctgattgtgctgaaggtac atatgatgtcaagtggtctgatgcgtttgtaagtgatacagacggacagaatatcacaagtaaggttactcttactgatggcgctatcattgttaag
Primer	M1-F	ggaggctcaggaggtggaggctccggaggtggaggctcaggtggtggtagtacaccgct
Primer	M2-F	caccaaaaaggagaagatctggaggtggaggctcaggaggtggaggct
Primer	M3-F	catcatatgcctcctcctgctctgccaccaaaaaggagaagatct
Primer	M-R	gaattcggatccctcgagcggaggtgctgcacatgcaaaattg
Primer	Md-R	gcagagattacctatctagacggaggtgctgcacatgc
Primer	his-F	ggtaatacaccatgaatcacaaag
Primer	his-R	ctatctagagtggtggtggtggtggtggtcgacaagcttgaattcgg
Primer	pScf-F	cctcagatgggcagcagcggtaagcctatccctaaccctctcctc
Primer	pScf-R	gagaccttaattcgcttataagaataacatagcaacaccagc
Primer	pF-F	gacctcagatgggcagcagccatatgcagacaaatccctatgccc
Primer	pF-R	gtcagagagaccttaattcgctcacaagtcctcttcagaaatgagc
Primer	pM-F	ccatcagagacctcagatgggcagcagccatcatcatcatcatcacagc
Primer	pM-R	cagagagaccttaattcgctcagtggtggtggtggtggtgctcgag
Primer	pZM-F	ggcggccgccagcttacgtacatcatcatcatcatcacagcagcggcc
Primer	pZM-R	gtctaaggctacaaactcagtggtggtggtggtggtgctcgagttgg
Primer	pPIC9K-F	gcgaattaaggtctctctgacttagacatgactgttcctcagttcaag
Primer	pPIC9K-R	tgaggtctctgatggctgctgcccatgaattctacgtaagcttcagc
Primer	pPICZC-F	tgagtttgtagccttagacatgactgttcctcagttcaag
Primer	pPICZC-R	tacgtaagctggcggccgccgcggctcgaggtaccgatcc
Primer	qC-F	tcctgtttgcggaagacagcg
Primer	qC-R	tgttggtgttgctcccttggtc

Primer	qF-F	gtccgtttaccgtccgttct
Primer	qF-R	gcgctgtatagcctggaaca
Primer	qM-F	gcagaccacagtaacgacga
Primer	qM-R	cattgccgtctttcagtgcc
Primer	qGAPDH-F	gtggtcatcaaaccggactca
Primer	qGAPDH-R	caagaaggtcgtcatcactgctc

674

675 **Supplementary Table 3. Insertion copy number of genes of engineered *Pichia pastoris* SMD1168**

Strain	Gene	Copy number
***P. pastoris* SMD1168$_{His4::CipA-CBM-CipC-SED1}$**	CipA-CBM-CipC-SED1	22.13±1.14
***P. pastoris* SMD1168$_{His4::MHETase}$**	MHETase	17.71±0.99
***P. pastoris* SMD1168$_{His4::FAST}$**	FAST	15.20±0.38
***P. pastoris* SMD1168$_{His4::FAST-MHETase}$**	MHETase	18.19±0.72
***P. pastoris* SMD1168$_{His4::FAST-MHETase}$**	FAST	14.54±0.77

676

677

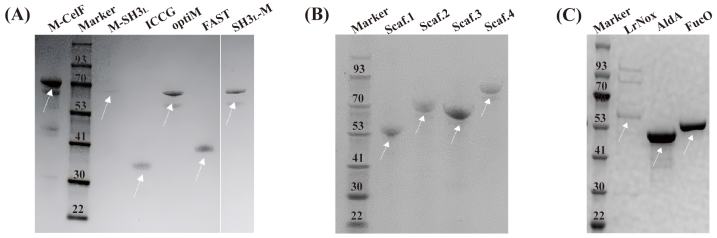

678 **Supplementary Fig. 1. SDS-PAGE of purified recombinant enzymes and protein scaffolds used in this study.**
679 **(A)** M-CelF: MHETase-CelF; optiM: codon optimized MHETase (as control); M-$SH3_L$: optiMHETase-$SH3_L$; $SH3_L$-
680 M: $SH3_L$-optiMHETase; ICCG: ICCG-ScaA; FAST: FAST-PETase-CelF. **(B)** Scaf.1: CipA-CipC; Scaf.2: CipA-
681 CBM-CipC; Scaf.3: CipA-CBM-$SH3_D$; Scaf.4: CipA-CBM-$SH3_D$-ScaB. **(C)** LrNox: LrNox-ScaA; FucO: FucO-
682 CelF; AldA: $SH3_L$-AldA. All proteins were Coomassie stained.

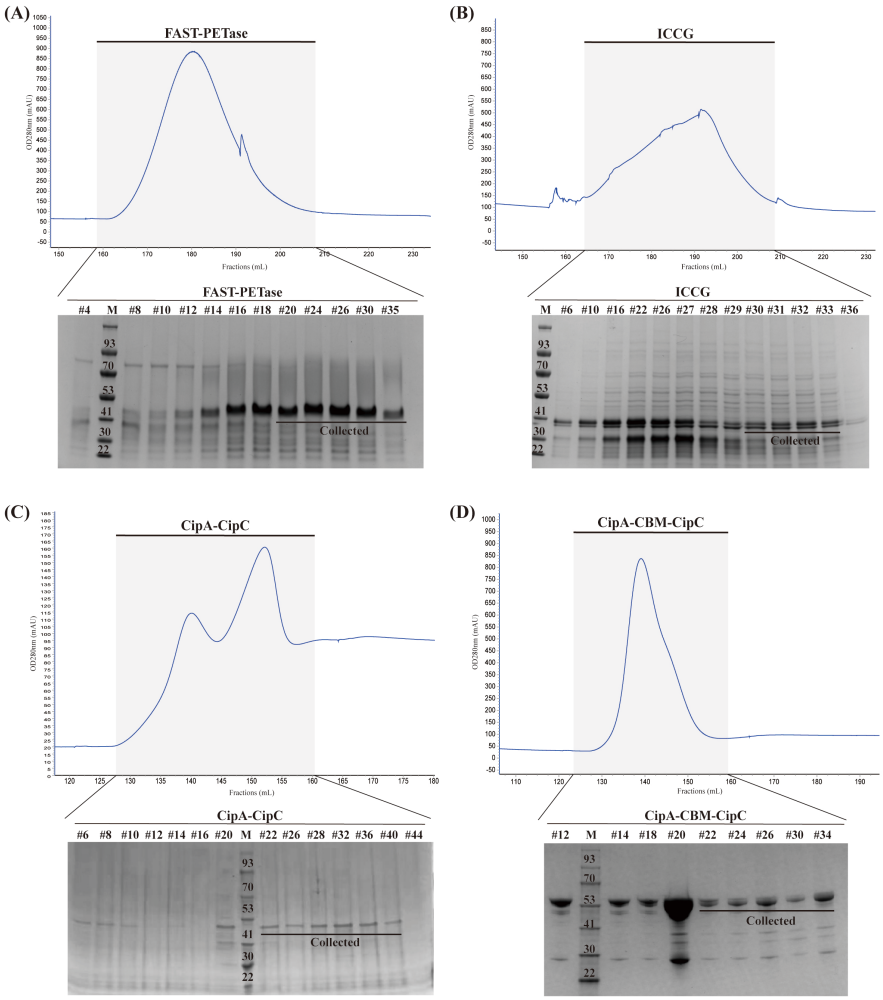

Supplementary Fig. 2. Purification of enzymes and protein scaffolds. (A)-(F) SDS-PAGE and Fast Protein Liquid Chromatography (FPLC) results of enzymes and scaffolds, followed by binding to HisTrap column and eluting the protein with high concentration of imidazole. **(A)** FAST-PETase-CelK. **(B)** ICCG-ScaA. **(C)** CipA-CipC (Scaf.1). **(D)** CipA-CBM-CipC (Scaf.2). **(E)** CipA-CBM-SH3$_D$ (Scaf.3). **(F)** CipA-CBM-SH3$_D$-ScaB (Scaf.4). M, marker; #4-#44, numbers of elution fractions from the HisTrap column.

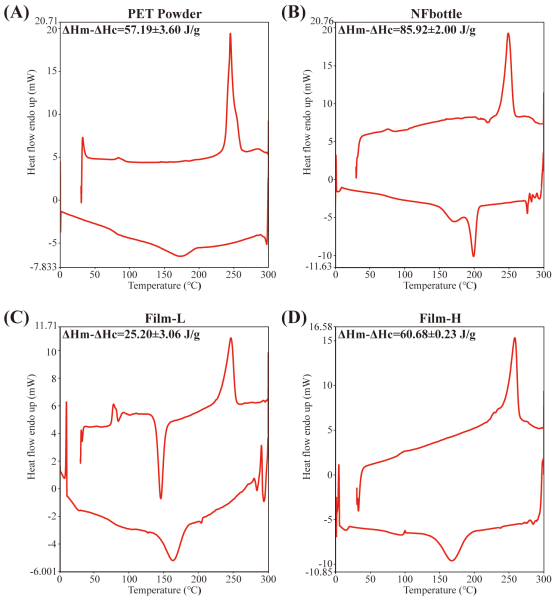

Supplementary Fig. 3. Crystallinity characterization of PET substrates used in this study. Differential scanning calorimetry (DSC) thermograms of different substrates: **(A)** PET powder (40.82% crystallinity). **(B)** NFbottle (61.33% crystallinity). **(C)** Film-L (17.99% crystallinity). **(D)** Film-H (43.31% crystallinity). ΔHm, heat of melting; ΔHc, heat of cold crystallization. Data are presented as mean ± s.d. (n = 3).

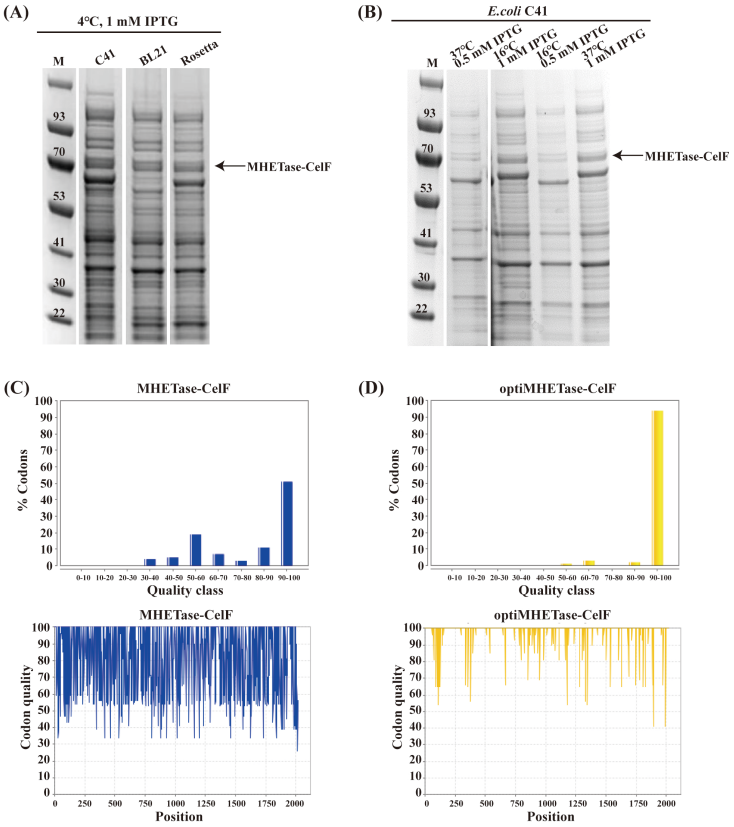

Supplementary Fig. 4. Optimizations of MHETase expression. (A) Optimization of strains for MHETase-CelF expression at 4°C, induced by 1 mM IPTG for 12 hours. SDS-PAGE result indicates the best strain *E.coli* C41(DE3) for MHETase expression. **(B)** Optimization of inducing conditions for MHETase-CelF expression. SDS-PAGE result indicates the best inducing condition, at 16°C, induced by 1 mM IPTG, for MHETase expression. M, Marker. **(C)-(D)** Condon quality distributions (top) and codon quality plot (bottom) of MHETases in *E.coli*. Results were calculated by GeneArt™ GeneOptimizer™ (Thermo Fisher). **(C)** MHETase-CelF (blue). **(D)** Codon optimized MHETase-CelF (optiMHETase-CelF, yellow).

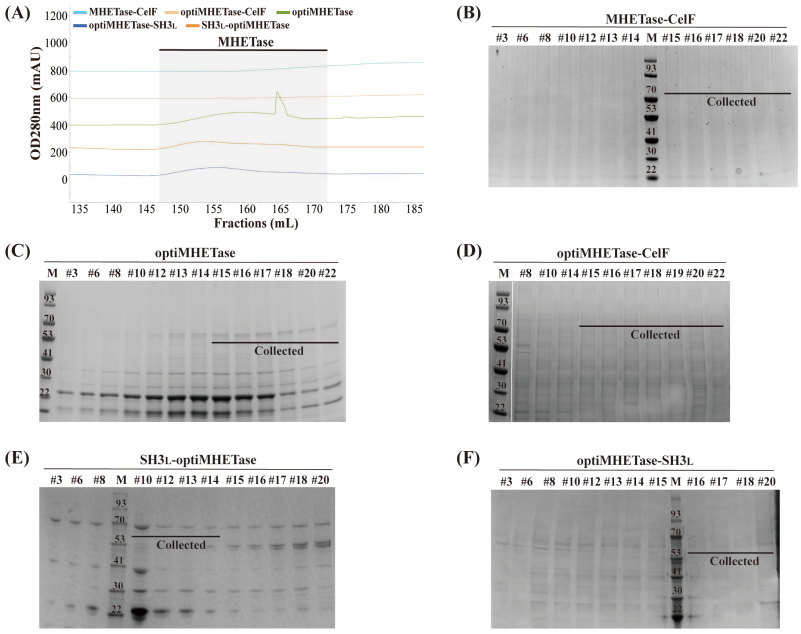

Supplementary Fig. 5. Purification of MHETases by Fast Protein Liquid Chromatography (FPLC). (A) Fast Protein Liquid Chromatography (FPLC) overlay results of MHETases. **(B)-(F)** SDS-PAGE of MHETases. M, marker; #3-#22, numbers of elution fractions from the HisTrap column.

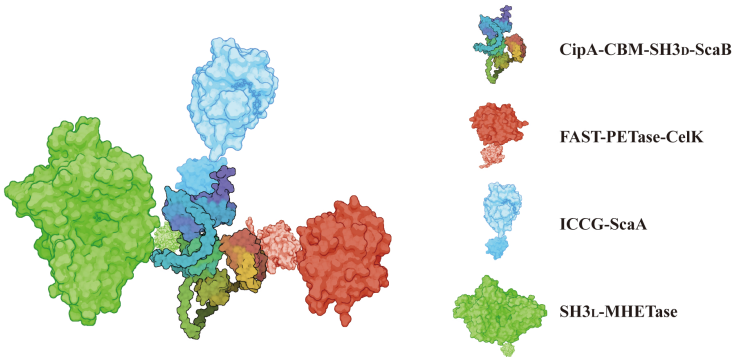

Supplementary Fig. 6. Predicted structure of enzyme-scaffold complex D. Structure of the scaffold, containing CipA (orange), CBM (brown), $SH3_D$ (green), ScaB (blue), was predicted by AlphaFold2.

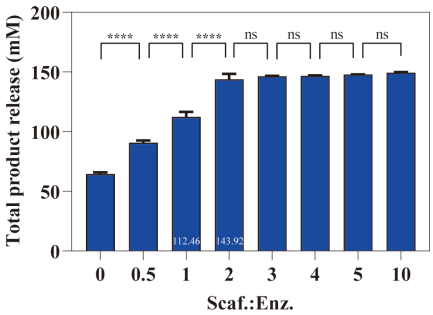

Supplementary Fig. 7. Optimization of enzyme-to-scaffold molar ratio in SPEED system. Effect of enzyme-to-scaffold molar ratio on PET degradation efficiency with fixed amount of enzyme (0.25 nmol individual enzymes). All reactions were performed at 30°C, pH 7.0, for 96 hours using 100 mg PET powder, with Scaf.4-to-enzyme molar ratio of .0:1/0.5:1/1:1/2:1/3:1/4:1/5:1/10:1.

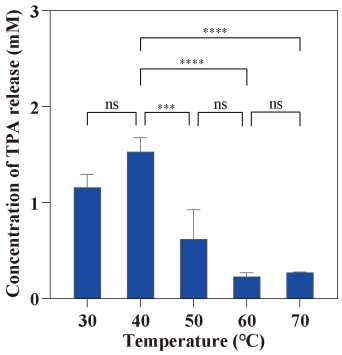

Supplementary Fig. 8. Assessment of optimal temperature of $SH3_L$-optiMHETase. The reaction was carried out by 0.5 mM enzyme with 5 mM MHET and BHET at pH 7.0 for 96 hours. The elevated TPA release observed in the 70°C group may be attributed to the self-degradation of the monomers under high temperatures (**Source Data**). Data are presented as mean ± s.d. (n = 3). Statistical significance was determined by one-way ANOVA (ns: not significant, *$p < 0.1$, **$p < 0.01$, ***$p < 0.001$, ****$p < 0.0001$).

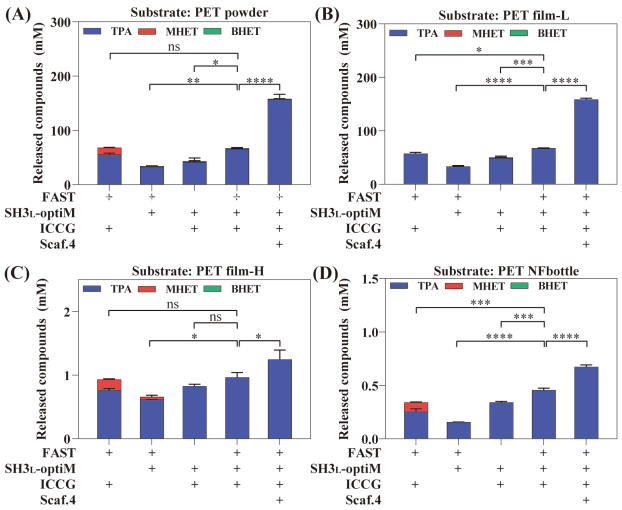

723

724 **Supplementary Fig. 9. PET degradation by SPEED Complex-D under optimal conditions.** PET degradation
725 assays of optimized Complex-D on different substrates: PET powder **(A)**, film-L **(B)**, film-H **(C)** and NFbottle **(D)**.
726 All reactions were performed at 40°C, pH 7.0, for 96 hours using 100 mg PET substrate, 0.5 nmol individual enzymes,
727 with an enzyme:scaffold molar ratio of 0.5:1. Data are presented as mean ± s.d. (n = 3). Statistical significance was
728 determined by one-way ANOVA (ns: not significant, *$p < 0.1$, **$p < 0.01$, ***$p < 0.001$, ****$p < 0.0001$).

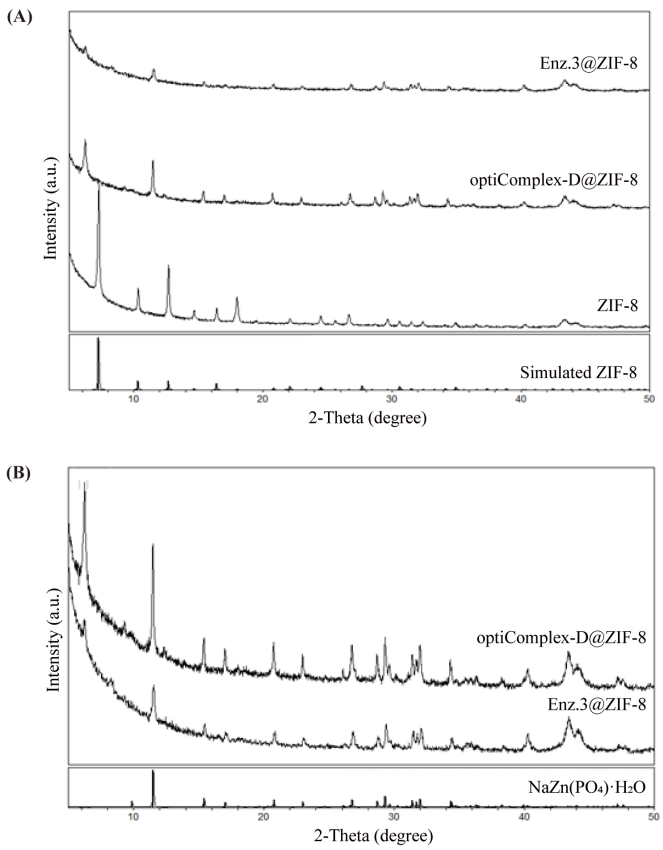

Supplementary Fig. 10. XRD spectra of immobilized samples. (A) XRD pattern simulated from CIF file of ZIF-8 (bottom, No. 00-062-1030), XRD patterns of synthesized ZIF-8, optiComplex-D@ZIF-8, and Enz.3@ZIF-8, respectively. **(B)** XRD patterns of simulated $NaZn(PO_4)\cdot H_2O$ (bottom), Enz.3@ZIF-8 and optiComplex-D@ZIF-8, respectively. Enz.3, FAST-PETase with ICCG and MHETase (0.25 nmol individual enzymes); optiComplex-D, Enz.3 with Scaf.4 (5 nmol).

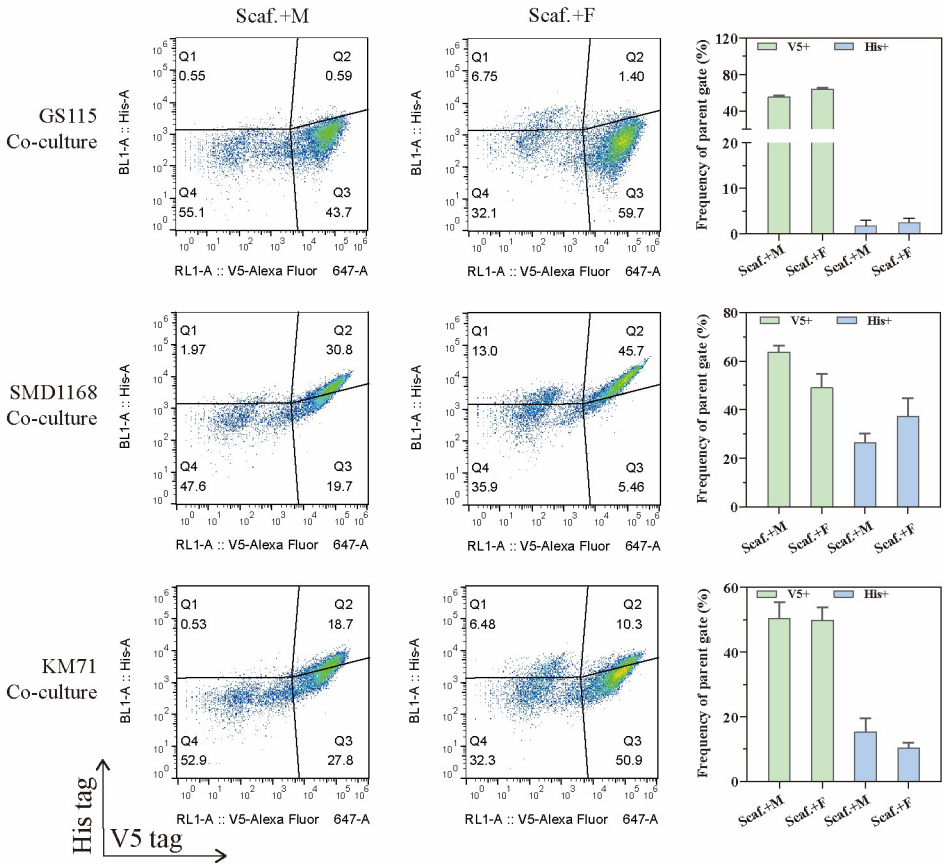

Supplementary Fig. 11. Scaffold expression and enzyme secretion assays in different *Pichia pastoris* strains. The scaffold (with V5 tag) displaying strain and enzyme (with His tag) secreting strains were pre-mixed and then induced at 30°C in BMMY medium. Scaf., *P. pastoris*$_{His4::CipA\text{-}CBM\text{-}CipC\text{-}SED1}$, M, *P. pastoris*$_{His4::MHETase}$, F, *P. pastoris*$_{His4::FAST}$. The scaffold was fused with V5 tag; MHETase and FAST were fused with his tag for detection. *P. pastoris*$_{His4::enzyme}$ was mixed with *P. pastoris*$_{His4::scaffold}$ in a 1:1 ratio, resulting in a final system comprising 2×10^7 *P. pastoris*$_{His4::scaffold}$.

Supplementary Methods

Calculation of total enzymes

Weight or the concentration of enzymes was got from corresponding paper (**Supplementary File 1**). Total enzymes amount was calculated with the sum of corresponding molar amount of single enzyme. For known weight of enzymes, molar amount of single enzyme was calculated with the formula below (molecular weight of each enzyme was calculated on https://web.expasy.org/protparam/):

$$Molar\ amount\ of\ single\ enzyme\ (nmol) = \frac{Weight\ (\mu g)}{Molecular\ weight\ (kDa)}$$

For known concentration of enzymes, molar amount of single enzyme was calculated with the formula below:

$$Molar\ amount\ of\ single\ enzyme\ (nmol) = \frac{Concentration\ (nM) \times Volume\ (mL)}{1000}$$

Calculation of total products

Weight loss or concentration of released total products was got from corresponding paper (**Supplementary File 1**). For known concentration of total products, molar amount was calculated with the formula below:

$$Molar\ amount\ of\ total\ products\ (\mu mol) = Concentration(mM) \times Volume(mL)$$

For known weight loss of total products, molar amount was calculated with the formula below (192 is the relative molecular mass of a bulding block of PET):

$$Molar\ amount\ of\ total\ products\ (\mu mol) = \frac{Weight\ loss\ (\%) \times Weight\ of\ PET\ (mg) \times 10}{192}$$

Calculation of degradation efficiency and improved fold-change

Degradation efficiency was calculated based on the above calculations, with the formula below:

$$Degradation\ efficiency\ (mol/mmol) = \frac{Molar\ amount\ of\ total\ products\ (\mu mol)}{Molar\ amount\ of\ single\ enzyme\ (nmol)}$$

Improved fold-change is the ratio of the above calculated degradation efficiencies (this study vs. previous study).

Calculation of percentage of recyclable monomer release

Percentage of recyclable monomer release was calculated based on the above calculations, with the

formula below:

$$Recyclable\ monomer\ release\ (\%) = \frac{Concentration_{TPA+EG}\ (mM)}{Concentration_{TPA+EG+MHET+BHET}\ (mM)} \times 100\%$$